



**João Carlos Moutinho
de Almeida**

**Metilação de DNA como potencial biomarcador da
Doença de Alzheimer**

**DNA Methylation as a potential biomarker for
Alzheimer Disease**



**João Carlos Moutinho
de Almeida**

**Metilação de DNA como potencial biomarcador da
Doença de Alzheimer**

**DNA Methylation as a potential biomarker for
Alzheimer Disease**

Dissertação apresentada à Universidade de Aveiro para cumprimento dos requisitos necessários à obtenção do grau de Mestre em Biomedicina Molecular, realizada sob a orientação científica da Professora Doutora. Ana Gabriela da Silva Cavaleiro Henriques, Professora Auxiliar Convidada da Secção Autónoma de Ciências da Saúde da Universidade de Aveiro

Este trabalho contou com o apoio do Centro de Biologia Celular (CBC) da Universidade de Aveiro, e é financiado por fundos FEDER através do Programa Operacional Factores de Competitividade-COMPETE e por Fundos nacionais da FCT no âmbito dos projetos PTDC/QUI-BIQ/101317/2008 e JPND-BIOMARKAPD.



Dedico em especial este trabalho aos meus avós, pessoas extraordinárias que me deram muito carinho, apoio e amor e que, apesar de já terem partido, estão sempre no meu coração...

o júri

presidente

Professora Doutora Odete Abreu Beirão da Cruz e Silva

Professora Auxiliar C/Agregação da Secção Autónoma de Ciências da Saúde, Universidade de Aveiro

Doutor Luís Filipe da Silva Godinho

Bolseiro de Pós-Doutoramento, Universidade de Aveiro

Professora Doutora Ana Gabriela da Silva Cavaleiro Henriques

Professora Auxiliar Convidada da Secção Autónoma de Ciências da Saúde, Universidade de Aveiro

agradecimentos

Quero agradecer à Professora Doutora Odete Abreu Beirão da Cruz e Silva por me ter acolhido no laboratório, por me ter possibilitado a realização deste trabalho e por todas as suas sugestões pertinentes.

Agradeço à minha orientadora, Professora Doutora Ana Gabriela da Silva Cavaleiro Henriques, pela forma como me tratou como pessoa, bem como, por todas as orientações dadas nas diferentes fases da tese, pelos ensinamentos, pelas correções, por todas críticas e pela motivação e apoio ao longo de todo este ano lectivo.

Agradeço ao Centro de Biologia Celular e à FCT.

Também queria agradecer a todos os elementos da equipa Gabi: Marta, Lili e Joana Oliveira por todo o apoio, ajuda e motivação. Um especial agradecimento para a Lili por toda a preciosa ajuda que me deu em todos os momentos deste trabalho.

Aos meus colegas de mestrado, em especial, aos colegas de bancada de laboratório, Sónia, Patrícia, Ana Maria, Catarina e Luísa pelo companheirismo, apoio e ajuda.

A todos os elementos do Laboratório de Neurociências, Mariana, Regina, Roberto, Pati, Filipa, Rocha... Um muito obrigado pelo bom ambiente e momentos divertidos.

Aos meus pais quero agradecer toda a educação, confiança, apoio, amor e carinho transmitidos ao longo destes vários anos. Ao meu irmão pelo apoio prestado, pela compreensão e, claro, por estar sempre a torcer por mim.

À Márcia queria agradecer por todo o carinho, apoio e dedicação todos os dias para que tudo me corra bem. Para ti um muito especial obrigado por me ajudares a crescer como pessoa e por me fazeres feliz...

Aos meus amigos gostava de agradecer toda a amizade e companheirismo que ajudaram em todo o percurso. Obrigado!

palavras-chave

Metilação de DNA; regiões promotoras de genes; envelhecimento; Doença de Alzheimer; CpG; hipometilação

resumo

A metilação de DNA é, de todos os mecanismos epigenéticos, o mais estudado e consiste na adição de um grupo metil ao carbono da posição 5 do anel de uma citosina. A metilação da região promotora de genes está diretamente relacionada com silenciamento genético, podendo conduzir ao desenvolvimento de determinadas patologias, uma vez que genes importantes não são expressos devido a este mecanismo. Este mecanismo epigenético tem vindo a ser estudado a nível do cancro e, recentemente, tem adquirido alguma importância ao nível de doenças neurológicas, como a doença de Alzheimer (DA). O envelhecimento é o maior factor de risco para a DA e ao mesmo tempo está na base de muitas das alterações nos mecanismos epigenéticos. Como a patologia e etiologia da DA ainda não é completamente conhecida, alterações ao nível de mecanismos epigenéticos, como a metilação de DNA, podem ajudar a entender as alterações de expressão de genes nesta doença.

Neste estudo, utilizaram-se amostras de pacientes com possível DA e controlos com idades semelhantes. O DNA genómico foi extraído de amostras de sangue e os níveis de metilação global foram avaliados por um ensaio de ELISA. Os pacientes apresentaram uma tendência para uma diminuição da metilação global ($0,75\% \pm 0,29$) relativamente aos controlos ($0,86\% \pm 0,29$). Os perfis de metilação dos genes envolvidos na DA, *APP* e *ApoE*, foram obtidos por *Combine Bisulfite Restriction Analysis* (COBRA), *Methylation Sensitive - High Resolution Melting* (MS-HRM) e *Bisulfite Direct Sequencing* (BDS). Para a região promotora do gene *ApoE*, não foram encontradas diferenças entre pacientes e controlos assim como a região promotora do gene *APP* não apresentou metilação através do método COBRA e MS-HRM. De igual modo, a região promotora do gene *ApoE* também não apresentou diferenças usando estas 2 técnicas. No entanto, a BDS evidenciou diferenças em locais CpGs específicos, mostrando que existe uma tendência para o aumento da metilação nos CpGs 1, 3 e 5; e para diminuição da metilação no CpG 6 dos pacientes relativamente aos indivíduos control. Este estudo permitiu verificar uma tendência para de diminuição da metilação global dos pacientes com possível DA relativamente aos controlos e também a existência de um possível padrão de metilação da região promotora do gene *ApoE*, que pode estar relacionado com a patologia da DA.

keywords

DNA methylation; promoter gene regions; aging; Alzheimer's Disease; CpG; hypomethylation

abstract

DNA methylation is the major studied epigenetic mechanism and consists in the addition of a methyl group to 5' carbon position of the cytosine ring. Methylation of promoter gene regions are directly correlated with gene silencing, which can allow the development of certain diseases since relevant genes may be inhibited due to its promoter methylation; being that the opposite can also occur. This epigenetic mechanism has been linked to cancer and recently it is also being pointed to have an important role in neurological disorders, such as Alzheimer's Disease (AD). Furthermore, aging is the major risk factor for AD, and also the process underlying many of the epigenetic alterations. As AD etiology and pathological development is not completely understood, alterations in epigenetic mechanisms like DNA methylation may underlie the basis of gene expression alterations.

Hence, in this study, possible AD patients and age- and sex-matched controls were used. Genomic DNA was extracted from blood samples and the global methylation levels were determined using an ELISA-type assay. The possible AD patients exhibit lower methylation levels ($0,75\% \pm 0,29$) than age- and sex-matched controls ($0,86\% \pm 0,29$). Gene specific methylation profiles of AD related genes, namely *APP* and *ApoE*, was carried out using Combine Bisulfite Restriction Analysis (COBRA), Methylation Sensitive-High Resolution Melting (MS-HRM) and Bisulfite Direct Sequencing. The *APP* promoter region did not reveal any methylation by COBRA and MS-HRM. For the *ApoE* promoter region evaluated no differences in the methylation levels could be detected between patients and controls using these two techniques. However, by sequencing analysis of this *ApoE* promoter region, differences arise in specific CpG sites, indicating a tendency for increased methylation of CpG1, CpG3 and CpG 5 and a decreased methylation of CpG6 in AD patients when compared with age- and sex-matched controls. In this study AD patients exhibited a tendency for lower global methylation levels when compared to control individuals and the *ApoE* promoter region exhibited a tendency for a pattern of methylation that maybe related to AD pathology.

Index

1. INTRODUCTION.....	1
1.1. Epigenetics.....	3
1.1.1. DNA methylation	4
1.1.1.1. Methylation in the promoter region	6
1.1.2. Histone modification	7
1.1.3. Nucleosome positioning and miRNA	8
1.2. Alzheimer Disease, the most common form of dementia.....	10
1.2.1. Epidemiology	11
1.2.2. Histological and molecular insights	11
1.2.3. Genetic component and Risk Factors for AD	14
1.2.4. Diagnosis of dementia	15
1.3. Epigenetic and Alzheimer's Disease	16
1.3.1. DNA methylation and AD	17
1.3.1.1. DNA methylation as a potential biomarker candidate	18
1.3.2. Epigenetic as a potential therapeutic target	19
2. AIMS OF THE STUDY	23
3. MATERIALS AND METHODS.....	27
3.1. Sample characterization.....	29
3.2. Genomic DNA extraction.....	30
3.3. Global methylation analysis	31
3.4. Bisulfite DNA modification	32
3.5. Selection of methylated gene region.....	34
3.6. Primer design	35
3.7. Combine Bisulfite Restriction Analysis	36
3.7.1. Amplification of <i>APP</i> and <i>ApoE</i> sequences by PCR.....	36
3.7.1.1. Agarose gel electrophoresis	38
3.7.2. Restriction Enzyme Selection and Digestion	38
3.8. Methylation-sensitive high resolution melting (MS-HRM)	40
3.8.1. High Resolution Melting (HRM) analysis	42
3.9. Direct Bisulfite Sequencing.....	42
4. RESULTS.....	45
4.1. Genomic DNA extraction from the sample group.....	47
4.2. Global methylation Levels in AD patients.....	48
4.3. Methylation Levels in AD associated genes	49
4.3.1. Restriction pattern of <i>APP</i> and <i>ApoE</i> genes in AD patients.....	49
4.3.2. Evaluation of <i>ApoE</i> and <i>APP</i> methylation levels by MS-HRM.....	52
4.3.3. Evaluation of <i>ApoE</i> methylation levels by sequencing analysis	56
5. DISCUSSION.....	61
Concluding Remarks	66

Studied Limitations and Future Perspective	66
6. REFERENCES	69
7. ANNEXES	85

Figure Index

Figure 1 - DNA Methylation cycle..	5
Figure 2 - Gene methylation in health and in disease..	7
Figure 3 - Annual incidence rate for AD.....	11
Figure 4 - Histopahtological hallmakrs of AD.....	12
Figure 5 - APP processing pathways.	13
Figure 6 - <i>ApoE</i> alleles..	15
Figure 7 – General steps for pure genomic DNA extraction from whole blood.	30
Figure 8 - Schematic representation of the Methylated DNA Quantification by ELISA.....	31
Figure 9 - Calculation of DNA methylation (5-mC) percentages.....	32
Figure 10 - Bisulfite conversion reactions.....	33
Figure 11 - CpG islands present in <i>APP</i> promoter region sequence.	35
Figure 12 – The <i>ApoE</i> promoter sequence.....	35
Figure 13 – Restriction recognition sites of HhaI in amplified <i>APP</i> sequence.	39
Figure 14 – Restriction recognition sites of SsiI in amplified <i>ApoE</i> sequence.	39
Figure 15 - Genomic DNA agarose gel electrophoresis.	48
Figure 16 - Dispersion graphic of global methylation percentages of possible AD patients and age- and sex-matched controls.....	49
Figure 17 - <i>ApoE</i> promoter sequence amplified by PCR.	50
Figure 18 - <i>APP</i> promoter sequence amplified by PCR.....	50
Figure 19 - Electrophoretic analysis of <i>ApoE</i> promoter sequence restriction by SsiI.	51
Figure 20 - Electrophoretic analysis of <i>APP</i> promoter sequence restriction by HhaI.....	52
Figure 21 – HRM curve generated by amplification of <i>ApoE</i> gene..	53
Figure 22 – HRM curve generated by amplification of <i>APP</i> region upstream TSS.....	54
Figure 23 - HRM curve generated by amplification of <i>APP</i> region downstream TSS	55
Figure 24 – <i>ApoE</i> bisulfite sequencing of methylated DNA control.....	57
Figure 25 – <i>ApoE</i> bisulfite sequencing of unmethylated DNA control..	57
Figure 26 - Results from bisulfite sequencing of APOE upstream TSS region.	58

Table Index

Table 1 - DNA methylation alterations in peripheral blood cells in neurodegenerative disorders.	19
Table 2 - Bisulfite conversion conditions.	33
Table 3 – Information about genes sequences according to UCSC Genome Bioinformatics.	34
Table 4 - Sets of primers used for <i>ApoE</i> and <i>APP</i> amplification for COBRA.	37
Table 5 – PCR amplification reaction composition.	37
Table 6 - PCR cycling conditions for <i>APP</i> gene amplification using Maxima HotStart.	37
Table 7 - PCR cycling conditions for <i>ApoE</i> gene amplification using Kappa Uracil+.	38
Table 8 - Enzymatic restriction mixture components.	40
Table 9 – Primers used in MS-HRM for methylation analysis of <i>ApoE</i> and <i>APP</i> .	41
Table 10 – PCR reaction for real-time amplification.	42
Table 11 – MS-HRM PCR program.	42
Table 12 - PCR conditions for PCR sequencing reaction.	43
Table 13 - NanoDrop results of samples genomic DNA.	47
Table 14 – Variant call results from HRM analysis.	56
Table 15 –Semi-quantitative analysis of CpG sites upstream <i>ApoE</i> TSS.	59

Abbreviations

5-hmC	5-hydroxymethylcytosine
5-mC	5-methylated cytosine
AD	Alzheimer's disease
AICD	APP intracellular domain
ApoE	Apolipoprotein E
APP	Amyloid precursor protein
A β	Amyloid- β
BACE1	β -site amyloid precursor protein cleaving enzyme 1
bDNA	Bisulfite modified DNA
C	Cytosine
CGI	CpG Island
CHD	Chromodomain helicase DNA-binding
COBRA	Combined Bisulfite Restriction Analysis
CSF	Cerebral Spinal Fluid
DLB	Dementia with Lewy Bodies
DNA	Deoxyribonucleic acid
DNMT	DNA methyltransferase
FTD	Frontotemporal Dementia
G	Guanine
HAT	Histone acetyltransferases
HCPs	High CG content promoters
HCY	Homocysteine
HDAC	Histone deacetylases
ICPs	Intermediate CG content promoters
ISWI	Imitation switch
K	Lysine
LCPs	Low CG content promoters
MC	Methylated Control
MBD	Methyl-CpG-binding domain
miRNA	MicroRNAs
MMSE	Mini-Mental State Examination (

MS-HRM	Methylation Sensitive – High Resolution Melting
ncRNA	Non-coding RNAs
NFT	Neurofibrillary tangles
NURF	Nucleosome remodeling factor
PSEN1	Presenilin 1
PSEN2	Presenilin 2
PTM	Post-transcriptional modification
R	Arginine
RISC	RNA-induced silencing complex
S	Serine
SAH	S-adenosylhomocysteine
SAM	S-adenosylmethionine
SP	Senile Plaques
SWI/SNF	Switch/Sucrose Nonfermentable
T	Threonine
TET	Ten-eleven translocation
TSS	Transcription Start Site
VaD	Vascular Dementia

1. Introduction

1.1. EPIGENETICS

Epigenetics can be defined as heritable changes in gene expression caused by modifications that do not involve alterations in deoxyribonucleic acid (DNA) sequence (1). Therefore, the term “epigenetic mechanisms” refers to the processes that modify gene expression without altering the genetic code itself. It includes covalent modifications of cytosine bases, namely DNA methylation; histones post-translational modifications, such as histones acetylation, phosphorylation or methylation; and changes in the nucleosomes positioning (2,3). These mechanisms play a key role in the regulation of many cellular processes, such as gene and microRNA expression, DNA-protein interactions, suppression of transposable element mobility, cellular differentiation, embryogenesis, X-chromosome inactivation and genomic imprinting (3).

The epigenetic marks can persist during development and potentially be transmitted to offspring, allowing the formation of many different phenotypes from the same genomic material (4). For example, monozygotic twins, although having the same DNA genomic sequence, have different DNA methylation and histone modification profiles which may contribute to the differences in the penetrance of several diseases, such as cancer or autoimmune disorders (5). Besides this, epigenetics seems to be one of the key factors in cellular differentiation that allows, for example, the stem cells to develop into any type of cell (6).

In the neurosciences field, the search for epigenetic modifications in the brain has pointed to the importance of this mechanism in development and disease, based on three evidences: the epigenome remains plastic throughout all periods of brain development and aging and that ongoing dynamic regulation occurs even in neurons and other postmitotic constituents of the brain (7–9); disordered chromatin organization and function have been pointed as playing key pathogenic roles in neurodevelopmental syndromes of early childhood and adult onset hereditary neurodegenerative disorders (10,11); and a variety of chromatin-modifying drugs had shown potential good results for a wide range of degenerative and functional disorders of nervous system (12–14).

Epigenetic modifications can be divided into three groups: DNA methylation, histone modifications and nucleosome positioning. These events are always present in the cells and the epigenetic outcome results from their interactions and feedback mechanisms (3).

1.1.1. DNA methylation

DNA methylation only occurs in the context of CpG dinucleotides, paired with the same sequence on the opposite DNA strand, and is the most widely studied epigenetic modification (3,15,16). The term “CpG” represents a cytosine (C) connected to a guanine (G) by a phosphodiester bond (3). The DNA strands can be methylated on both strands or only on one (hemimethylation), being the latter a transient stage during cell replication. The methylation patterns are copied between cell division by the DNA methyltransferase 1 (DNMT1), which only methylates DNA strand hemimethylated sites, leaving unmethylated the previous unmethylated DNA sites (15). The CpG dinucleotides tend to be found in regions called CpG islands (CGIs) that by definition are regions with more than 200 bases, with a G+C content more than 50% and a ratio of observed statistically expected CpG frequencies of at least 0,6 which can be calculated by this formula $((\text{Num of CpG}/(\text{Num of C} \times \text{Num of G})) \times \text{Total number of nucleotides in the sequence})$ (17).

In mammals, most of cytosine methylation occurs in the context of CG dinucleotide (18). The enzymes family DNA methyltransferases (DNMTs) are responsible for catalyzing the transference of a methyl group, from S-adenosyl methionine, to the 5' carbon position of the cytosine ring from DNA, resulting in its methylation (19). There are 5 members of the DNMT family but only DNMT1, DNMT3a and DNMT3b have methyltransferase activity (3). These 3 enzymes can be divided in 2 classes according to their function: maintenance DNMT, such as DNMT1; and *de novo* DNMT, like DNMT3a and DNMT3b (3). For example, DNMT3a, along with its cofactor DNMT3-like, are active in sexual stem cells and are responsible for introducing DNA methylation in these cells during oogenesis or spermatogenesis. The new methylation occurs in CpG Islands contained in the promoter of imprinted genes and is responsible for their silencing, originating a long term epigenetic stability (20,21). On the other hand, DNMT1 can exist in two forms: DNMT1o, the oocyte form of DNMT1; and DNMT1s, the somatic form. The DNMT1o acts only in the first division after fertilization, by maintaining the methylation of differentially methylated imprinted genes regions, during pre-implantation development (22). In the subsequent divisions instead of DNMT1o, DNMT1s is active and maintain the methylation through embryonic and adult tissues cells division. DNA-methylation patterns are somatically heritable due to the action of DNMT1 which has a low error rate of maintaining methylation (approximately 1% per division) (23).

Although DNMTs are commonly divided in maintenance DNMTs and *de novo* DNMTs, this distinction not always apply with both class of enzymes being involved in *de novo* and

maintenance methylation (24). Unlike DNMT3b that encodes multiple variants via alternative splicing, DNMT3a has only two isoforms, Dnmt3a and Dnmt3a2, which have different DNA targets and functions in development (25).

The methylation of DNA requires a component to provide a methyl group. This methyl group donor is not restricted to DNA methylation but also intervenes in other reactions that involve methylation, such as histone methylation. In all organisms, s-adenosylmethionine (SAM) is the primary methyl donor for processes that involves methylation of molecules (Figure 1) (26).

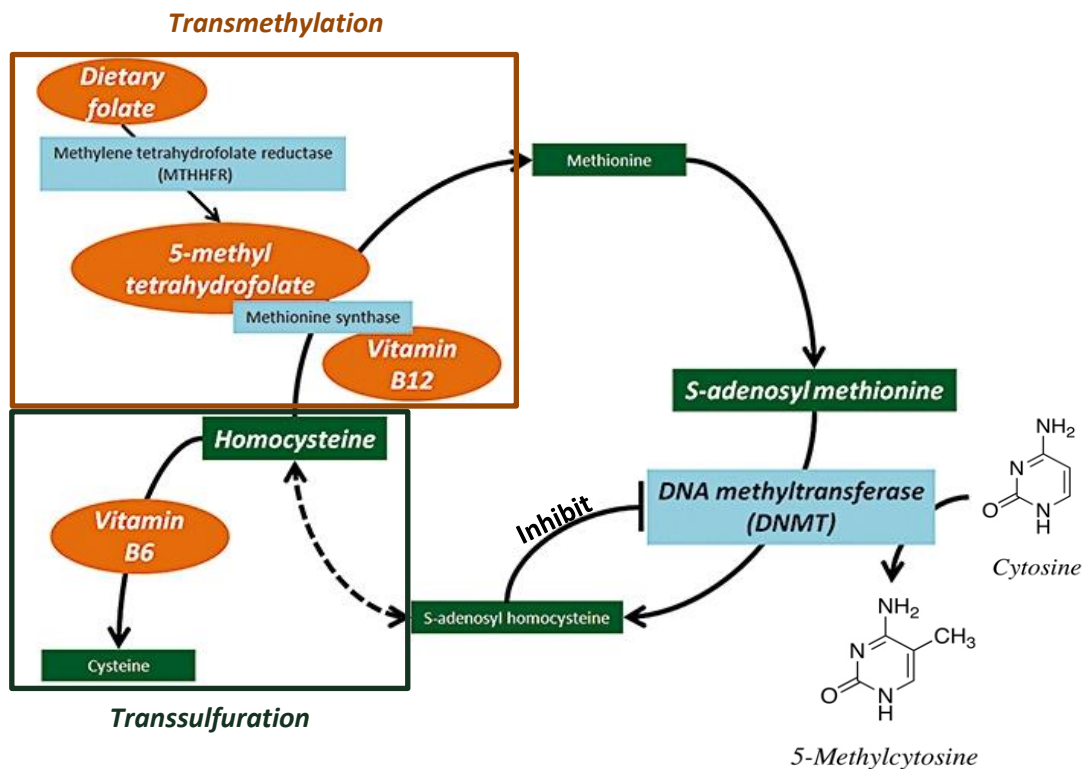


Figure 1 - DNA Methylation cycle. The methionine is acquired through diet or from the folate metabolism and due to the action of methionine adenosyltransferase forms SAM. DNMTs transfer a methyl group from SAM to carbon in position 5 of cytosine ring, originating methylcytosine. As SAM loses a methyl group, another compound called S-adenosylhomocysteine (SAH) is formed, whose high levels are responsible for inhibiting DNMTs activity. SAH is hydrolyzed by SAH hydrolase and forms homocysteine (HCY). HCY can be either subjected to transsulfuration, originating ultimately glutathione, an anti-oxidant agent from cysteine; or undergo transmethylation, catalyzed by Methionine synthase, which consists in the transference of the methyl group to HCY, originating methionine. The transsulfuration and transmethylation pathways need adequate levels of vitamin B6 and vitamin B12 that act as cofactors preventing methionine from being converted back to SAH and HCY, respectively. Adapted from (27).

DNA methylation leads to gene silencing mainly by two modes of action: recruitment of repressors that recognize and bind to 5-methylcytosines, called methyl-CpG-binding domain

(MBD) proteins; or, by direct interference with the transcription-factor binding, thus preventing the interaction between the DNA-binding protein and their specific DNA sites (28). In mammals, there are five well characterized MBD proteins: methyl CpG binding protein 2 (MeCP2), MBD1, MBD2, MBD3 and MBD4; which are responsible for recruiting histone-modifier genes, resulting in transcriptionally inactive chromatin (29,30).

The recent discovery of 5-hydroxymethylcytosine (5-hmC), which results from hydroxylation of 5-methylated cytosine (5-mC) by ten-eleven translocation (TET) proteins, has raised the possibility of an intermediate epigenetic state associated with changes in DNA methylation and transcriptional regulation during development, normal and disease states (31–33). Although little is known about 5-hmC, several studies showed abundant levels of this modified base in pluripotent cells and neurons. Therefore, as 5-mC is considered the “fifth base” of DNA, 5-hmC has been pointed to be the “sixth base” (34,35).

1.1.1.1. Methylation in the promoter region

A gene promoter can be defined as a DNA sequence to which ribonucleic acid (RNA) polymerase binds to initiate gene transcription (36). According to CG density, promoters can be divided into 3 classes: low CG content promoters (LCPs), intermediate CG content promoters (ICPs) and high CG content promoters (HCPs) (18). Approximately 70% of all genes in the human genome have within them CGIs as well as about 50% of transcription start sites (TSS), which are considered the +1 position (18,36). The TSS represents the first nucleotide of first codon transcribed into RNA molecule, whose exact position is crucial for the identification of the regulatory regions that immediately flank it (37).

In a normal state, HCPs tend to be unmethylated and related to housekeeping and specific well regulated developmental genes. In many hypomethylated HCPs, gene expression can be inactivated or non-productive, despite the normal action of RNA Polymerase II, and also show high levels of dimethylation of Lys4 of histone H3. In contrast, genes with LCPs are usually hypermethylated in somatic cells, and associated with tissue specific genes or with other genes required for their activation (18).

However, when promoter methylation patterns are altered, chromatin conformation is altered, affecting directly gene expression, which can result into a disease development (Figure 2). Hypomethylation is intimately related with gene aberrant expression, whereas, hypermethylation has a silencing effect. These changes can occur either in promoters with CGIs or promoters not containing it, namely in CGI shores. The CGI shores can be defined as regions with lower CpG

density that lie in close proximity, but not within CGIs, and, therefore, its methylation have direct impact in gene expression, more precisely by silencing it (35,38).

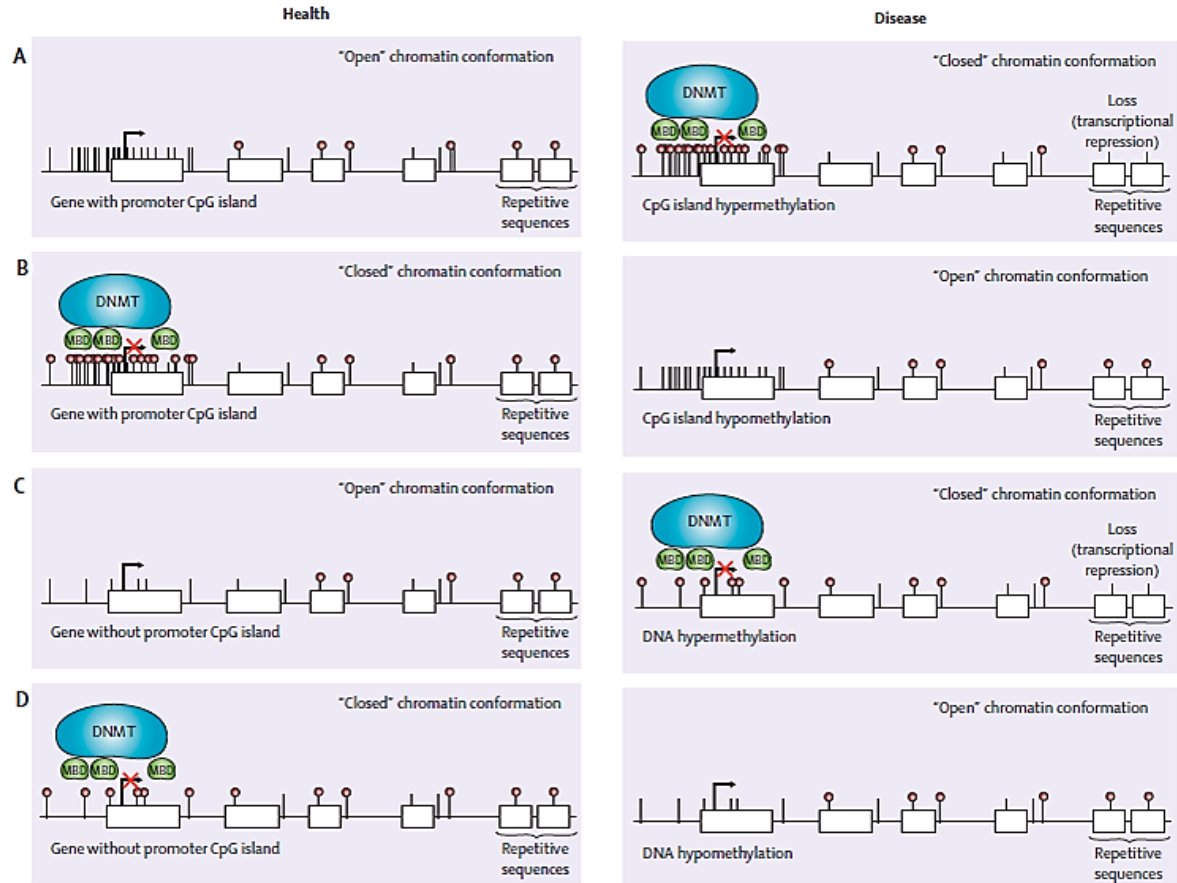


Figure 2 - Gene methylation in health and in disease. Alterations in promoter methylation patterns determine an open or closed chromatin conformation. Genes that do not have methylation in their promoters can become hypermethylated in pathological conditions (A), leading to silencing of genes naturally expressed. On the other hand, genes naturally silenced by methylation, can start to be pathologically expressed if methylation is lost (B). Furthermore, the same consequence can be observed in CpG island shores, whose methylation patterns alterations can lead to pathological transcriptional repression (C) or pathological gene expression (D). Reproduced from (30).

1.1.2. Histone modification

The nucleosome is composed by core histones, such as H2A, H2B, H3 and H4, which are grouped into two dimers of H2A-H2B and one H3-H4 tetramer; and a 147-bp segment of DNA wrapped in 1,65 turns around the histone octamer (39). Two consecutive nucleosomes are separated by approximately 50bp of free DNA. Histone H1 is not a part of the nucleosome, but it has an important function, by binding to linker DNA and ensuring the right location of nucleosomes. The core histones are predominantly globular, exhibiting unstructured N-terminal tails (40). All histones undergo post-transcriptional modification (PTM), mainly in their tails, such

as acetylation, methylation, phosphorylation, ubiquitination, sumoylation and ADP-ribosylation, which are important in transcriptional regulation, chromosome condensation, DNA repair, DNA replication and alternative splicing (41,42). Acetylation, ubiquitylation and sumoylation occur mainly in lysine (K) residues; whereas methylation affect arginine (R) and K residues; and phosphorylation occurs at serine (S) and threonine (T) residues (43). This is a reversible and dynamic process that involves the action of two antagonistic enzymatic complexes, responsible for adding or removing specific chemical group in specific sites (30). Usually, the nomenclature of PTM histones is the histone, followed by residue and its position and finally the PTM occurred, for example, acetylation of H3 in lysine residue in position 27 is represented by H3K27ac.

The acetylation of lysine residues in the tail of histone is the most studied PTM and is associated with active transcriptional activity. In this PTM, the enzymes responsible for the attachment of an acetyl group to the histone tail are called histone acetyltransferases (HATs), while histone deacetylases (HDACs) are responsible for reverting it (40). HATs regulate gene transcription by interaction with transcription factors. HDACs have sequence specificity action since they depend on the recruitment by repressors, co-repressors and methyl-DNA binding proteins (44).

According with the transcriptional levels, the human genome can be divided into euchromatin, with intense transcriptional activity; and heterochromatin, which is transcriptionally inactive. The first one shows high levels of acetylation, like in H3K27ac and H2BK5ac (promoter region), and usually H3 trimethylation in lysine residues of H3K4, H3K36 and H3K79; while heterochromatin exhibits low levels of acetylation and high level of methylation in H3K9, H3K27 and H4K20 (45).

1.1.3. Nucleosome positioning and miRNA

The way like DNA is wrapped in nucleosomes interfere with the transcription process and, therefore, can affect all steps of gene expression regulation, as their/nucleosomes positions are able to prevent the activity of activator and transcription factors, affecting the elongation of RNA polymerase. Nucleosomes position at TSS is crucial for the initiation of transcription, once the presence and loss of nucleosome within the TSS is related to gene repression and activation, respectively (3). Despite controlling the accessibility of transcription factors to target DNA regions, disposition of nucleosomes directs meiotic recombination events and regulates methylation patterns, while chromatin remodeling is influenced by histone variants incorporated in DNA and DNA methylation (46,47).

There are 4 families of complexes, known as chromatin remodeling complexes that are responsible for all events regarding nucleosomes. All of these complexes rely on ATP hydrolysis, comprise an ATPase domain, and differ only in the composition of their unique subunits. The Switch/Sucrose Nonfermentable (SWI/SNF) family complexes have been proved to be regulators of gene expression and participate in alternative splicing [Reviewed in (48)]. The imitation switch (ISWI) family is associated with chromatin assembly and transcription repression, with only one exception complex, nucleosome remodeling factor (NURF) that participates in transcriptional activation. The third group is chromodomain helicase DNA-binding (CHD) family that is not only involved in the sliding and ejection of nucleosomes (gene expression), but can also have repressive activity, when the complexes have histone deacetylase activity and methyl-CpG-binding domain proteins. The last family, designated as INO80, participates in a variety of cellular processes such as transcription activation, DNA repair and replication, telomere regulation and chromosome segregation. A member of this last family, SWR1 is capable of replace H2A-H2B dimers with H2A.Z-H2B dimers [Reviewed in (49,50)].

MicroRNAs (miRNAs) are also able to regulate chromatin remodeling through the interaction with complexes responsible for it, more precisely, mediating the specific subunits changes (51). Despite this action, miRNAs also control histone variant replacement. The miRNAs are RNA molecules, usually composed by approximately 22 nucleotides, whose function is to participate in gene expression regulation (52). There are two ways by which miRNAs can operate: they can bind to mRNA target with total complementarity and lead to its complete degradation; or bind to a less complementarity region, such as 3' UTR regions, and suppress translation of the target gene [Reviewed in (53,54)]. Therefore, one miRNA can have multiple target regions and can interfere with regulation of multiple different genes (55,56).

microRNAs are members of non-coding RNAs (ncRNAs) and result from the processing of a long primary transcript, with one or more precursor miRNAs; or short hairpin introns by direct intron splicing, although this last is only for a subset of miRNAs. These processes result in the formation of pre-miRNAs with a length usually between 70-100 nucleotides, which are routed towards the cytoplasm by the karyopherin exportin-5. In the cytoplasm, pre-miRNAs are processed by endonuclease RNase III Dicer and RNA helicase, resulting in a single strand mature miRNA that is later assembled to the RNA-induced silencing complex (RISC). Although miRNAs are an area with much to be discovered, it is known that the major responsible for the transcription of miRNAs is RNA polymerase II, in what concerns the tissue specific genes allowing their spatially

and temporally regulation. The housekeeping ncRNA genes expressed in all types of cells have their transcription through RNA polymerase III [Reviewed in (57)].

The miRNAs may contribute to DNA methylation since all enzymes responsible for DNA methylation DNMT1, 3a and 3b are predicted to be miRNAs targets (52). Furthermore, DNA methylation and histone modification can affect miRNAs expression (58). Also, miRNAs are possible to be regulated by specific promoters that can be contained within CpG island and, therefore, DNA methylation maybe one process that might regulate miRNAs expression (59).

Epigenetic regulation of gene expression has a major importance in rapid cell adaptation to environmental conditions changes during life and across multiple generations. In brain, these mechanisms allow brain plasticity in response to experiences during lifetime. Although epigenetic mechanisms allow adaptive responses to positive and beneficial experiences, adverse environmental conditions can also induce neuronal responses that may culminate in pathological processes. Neuronal plasticity and susceptibility to neurological disease are dependent on experience and environment conditions (60,61).

1.2. ALZHEIMER DISEASE, THE MOST COMMON FORM OF DEMENTIA

Alzheimer's disease (AD) is the major cause of dementia in the elderly (62). The diagnosis of AD is most often based on the criteria from the National Institute of Neurologic and Communicative Disorders and Stroke – Alzheimer's Disease and Related Disorders Association (NINCDS-ADRDA) which can result in three kinds of diagnosis: **definitive**, which has a clinical diagnosis with histologic confirmation; **probable**, characterized by typical clinical syndrome without histologic confirmation; and **possible**, when the patient presents atypical clinical features but no alternative diagnosis apparent without histologic confirmation (63,64). The classical clinical features of AD are an amnesic type of memory impairment, deterioration of language, and visuo-spatial deficits (65). In late phases of the disease patients may exhibit motor and sensory abnormalities, gait disturbances and seizures (64).

Alzheimers disease is a complex neurodegenerative disorder characterized by two forms of the disease: a familial form (early-onset incidence) that is rare and follows Mendelian

inheritance; and a sporadic or idiopathic form (late-onset incidence), which is the most common form of this dementia (66). Regarding the typical pathological hallmarks of the disease, there are no differences between sporadic and familial AD forms (67,68).

1.2.1. Epidemiology

According to several studies, approximately 4,6 million new cases are known every year and, at age of 60, North America and Western Europe exhibit the higher prevalence numbers for AD (69). For population with age above 65 years old, the prevalence of dementia, predominantly AD, increases exponentially almost 15-fold as well as the annual incident rate (

. The incidence rates of AD are difficult to determine accurately due to two factors: the determination of the exact onset age and the establishment of a study population without this disease (70,71). In Portugal, it is estimated that 153 000 persons suffer from dementia, in which AD is the cause of 90 000 cases (72).

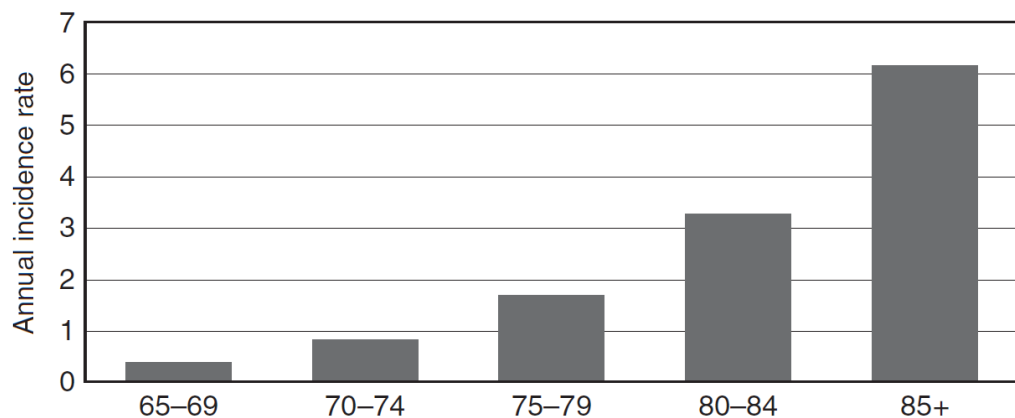


Figure 3 - Annual incidence rate for AD. Adapted from (70).

1.2.2. Histological and molecular insights

Although the macroscopic alterations in the brain do not allow the diagnosis of AD patients, because they are not limited to AD patients, the histological examination of the post mortem brain tissue samples can determine a definitive diagnosis of AD (73). Histological analysis of AD brain tissue shows the presence of senile plaques (SPs), neurofibrillary tangles (NFTs) and extensive neuronal loss in specific brain regions (Figure 4) (65).

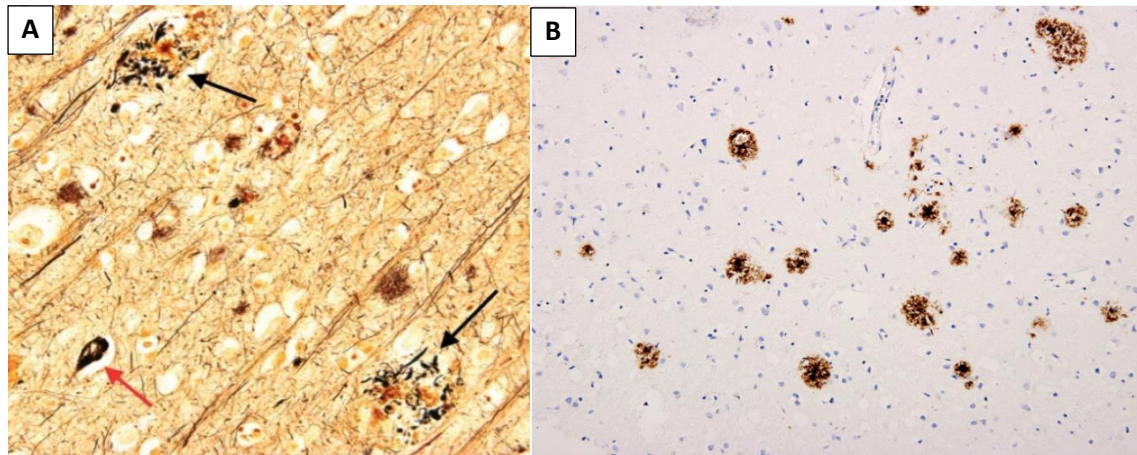


Figure 4 - Histopathological hallmarks of AD. Histological samples of temporal cortex of an AD patient showing SPs (black arrows) and NFTs (red arrow) by modified Bielschowski stain (A) and aggregates of A β (component of senile plaques) stained with an antibody directed against the components of A β (B). Adapted from (73).

The neuropathological features of AD brain encompass abundant SPs and NFTs, the later containing hyperphosphorylated tau; dramatic loss of synapses and neurons in the hippocampus and cerebral cortex; dystrophic neuritis astrogliosis; and microglial cell activation (68,74). All of these features have specific distributions, for example the SPs are found throughout the cortical mantle but NFTs are primarily found in limbic and association cortices(75,76).

The main element of SPs is the amyloid- β (A β) peptide, which is a peptide with 38-43 aminoacids originated from cleavage of the amyloid precursor protein (APP) (68,77). The exact role played by APP in a physiological manner is yet to be clarified, although it is known that APP participates in a variety of processes, such as cell growth, motility, neurite outgrowth, synapse formation (synaptic scaling and synaptic vesicle release), neural plasticity and cell survival (78). APP is the only protein of its family whose cleavage originates an amyloidogenic fragment. APP transcript can generated up to 8 isoforms through alternative splicing, including one isoform with 695 amino acids, which is mainly expressed in the central nervous system (CNS)(79).

The APP can be processed through a variety of pathways, some of which originate peptide A β (Figure 5) (78). At the cell surface, APP can be processed in an amyloidogenic or nonamyloidogenic pathway. The first pathway encompasses the cleavage of APP first by β -secretase followed by γ -secretase, resulting in the production and release of the A β peptide, whose most common isoforms have 40 and 42 amino-acids. The A β suffers complex conformational changes, aggregating and originating soluble fragments and oligomers, with highly neurotoxic effects. As A β is continuously produced and accumulated, the soluble fragments and oligomers transit to large fibrils which are then deposited into SPs (68,78). Due to the higher degree of fibrilization and insolubility, A β 42 is the most common isoform present in SPs (74). In

the nonamyloidogenic pathway α -secretase cleavage precludes A β formation, releasing instead a fragment followed by γ -secretase cleavage, called p3. The p3 fragment has low aggregation capacity and is not able to form oligomers. The γ -secretase is a multiprotein complex responsible for the sequential intramembranous proteolysis of multiple transmembrane proteins, which is constituted by presenilin 1 (PSEN1) or presenilin 2 (PSEN2), nicastrin and two multipass transmembrane proteins (Aph-1 and Pen-2) [Reviewed in (80)]. Along with p3 and A β fragments, another fragment, called the APP intracellular domain (AICD), is also released. The AICD is responsible to facilitate the interaction of APP with various cytosolic proteins that regulate APP's intracellular trafficking and/or signal transduction function; it has also been reported to possess transactivation activity and regulatory functions, being able to regulate transcription of multiple genes including APP, glycogen synthase kinase 3 (GSK-3 β), β -site amyloid precursor protein cleaving enzyme 1 (BACE1); as well as, induction of apoptosis [Reviewed in (81)].

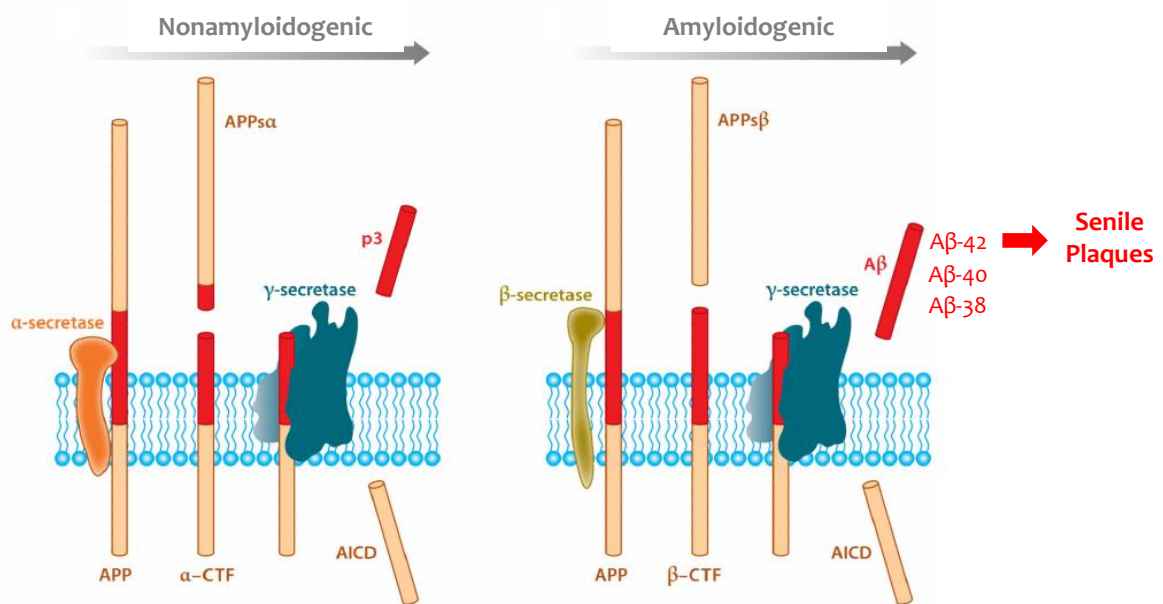


Figure 5 - APP processing pathways. The p3 fragment, originated via nonamyloidogenic processing, has poorer aggregation properties in comparison with A β that is responsible from SPs formation. Adapted from (78)

The NFTs are essentially composed by the microtubule associated protein tau, which has a very important role in stabilizing structure of microtubules. In the NFTs, tau is abnormally hyperphosphorylated and aberrantly misfolded (74). Three stages can be defined according with NFTs formation and cellular distribution: first, **pre-NFTs** characterized by a diffuse, and sometimes punctuate, pattern present in normal neurons with normal morphology; secondly, fibrillar **intraneuronal NFTs**, that result from aggregation of tau protein into cytoplasmic filaments,

observed in neurons with misplaced nucleus and distorted-appearing dendrites; and third, **extraneuronal NFTs** that consists of NFTs released into extracellular compartment due to the death of neurons with intraneuronal NFTs. The severity and duration of dementia have been correlated with the extent and distribution of NFTs. However the exact role of NFTs in AD is unclear, remaining two hypothesis: NFTs as a pathological mechanism and precursor of neuronal death in AD or as a neuroprotective mechanism in order to diminish neuronal damage (82,83).

1.2.3. Genetic component and Risk Factors for AD

The early onset of AD accounts for about 5% of all diagnosis of AD, affecting people below 65 years, with a familial history and an autosomal dominant transmission pattern (66). This form is associated with mutations in the genes of *APP*, *PSEN1* and *PSEN2* (84–86). However not all early-onset AD patients have mutations in this 3 genes, indicating that another mechanism may be also responsible for it (87).

Until now, 33 pathogenic mutations in *APP* gene have been described (<http://www.molgen.vib-ua.be/ADMutations/default.cfm?MT=0&ML=1&Page=AD>). These mutations can either be a duplication of the gene segment or a point mutation in the promoter region, resulting in the increase of wild-type protein or mRNA levels, respectively. The *PSEN1* is a conserved polytopic membrane protein that mediates the γ -secretase cleavage of APP, and mutations in this gene result in increased A β production (88). Since discovery of this gene, the number of described mutations is increasing, being more than 180 so far. Mutations in *PSEN2* have been also found but, despite its significant homology with *PSEN1*, the result of its mutations is less severe and the age of onset is usually higher. Furthermore, the disease progression is slower than what is observed in *APP* and *PSEN1* mutations. These 3 genes belong to the same biochemical pathways that results in the alterations of A β production, increasing the abundance of A β -42 species and, consequently, SPs. However, several familial early-onset AD are not related to mutations in any of the genes above mentioned, underlying the role of other candidate proteins involved in APP processing or other mechanism yet to be discovered (66).

On the other hand, late onset AD encompasses 95% of all AD cases and don't exhibit any familial disease history and, therefore, is very complex. The only high risk factor proved this far to be associated with AD is apolipoprotein E (ApoE) (89). There are three major alleles of *ApoE* locus that result from combinations of two amino acids changes in 112 and 158 residues of protein (Figure 6). The *ApoE* **allele ϵ 2** encodes Cys at 112 and 158 residues; the **allele ϵ 3** originates Cys at residue 112 and at 158 an arginine; and **allele ϵ 4** which encodes arginine in both residues. Large

studies have proved the higher risk to develop AD in patients with $\epsilon 4$ presence (90). In contrast, studies pointed to a protective action of $\epsilon 2$ (87). However, it is important to highlight that *ApoE* $\epsilon 4$ does not reflect *per se* the development of AD, but it increases the predisposition to it.

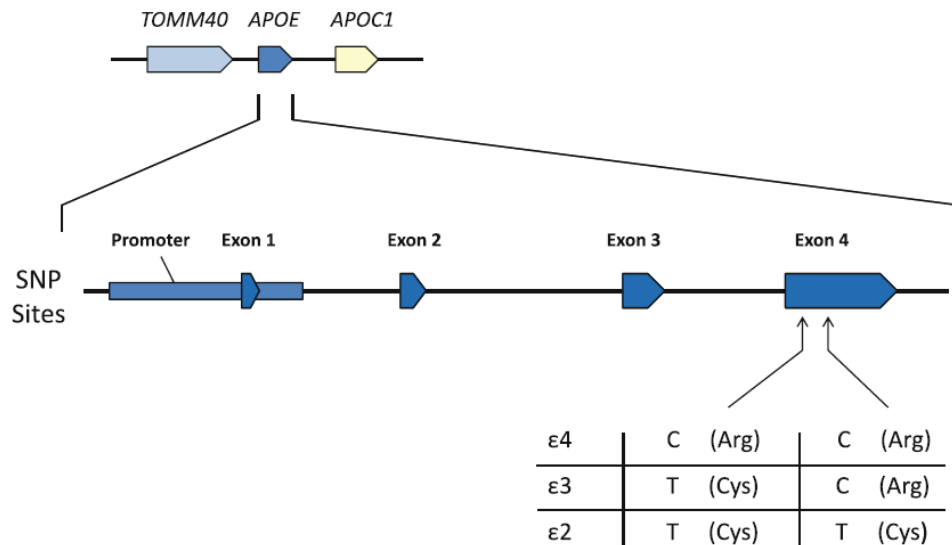


Figure 6 - *ApoE* alleles. Nucleotide alterations in exon 4 of *ApoE* gene are responsible for the three *ApoE* alleles, determining the encoded amino acid in 112 and 158 residues. The *ApoE* allele $\epsilon 4$ carriers have increased risk of developing AD. Reproduced from (87).

1.2.4. Diagnosis of dementia

Since many dementing disorders exhibit higher overlap degree of symptomatology, pathological and molecular pathways, the differential diagnosis among pathologies is sometimes difficult. The differential diagnosis is done by clinical evaluation that includes and combine information from cognitive and behavior assessment, neuroimaging findings, genetic tests and levels of certain proteins in cerebral spinal fluid (CSF).

The clinical diagnose of dementia is mainly based on medical history and cognitive evaluation for exclusion of other dementias and to target to more specific examinations. At early stages of dementia, specific patterns of cognitive and behavioural dysfunctions reflect disruption of specific brain regions and structures. Among the most commonly used cognitive screening tool is Mini-Mental State Examination (MMSE) (91). The MMSE is a 30-point test of cognitive function that contains tests of attention working memory, episodic memory (orientation and recall), language comprehension, visual-spatial functions, naming and copying. The MMSE should be complemented with other neuropsychological tests such as DemTect or clock drawing test, as several AD and mild cognitive impairment patients exhibit normal MMSE scores (92,93). Non-cognitive symptoms of dementia, such as apathy, psychosis, affective and hyperactive behaviours,

should also be assessed, using for example geriatric depression scale (94); not only because they are supportive features in the diagnosis of non-AD dementias like Dementia with Lewy Bodies (DLB), Parkinson's Disease with Dementia and Frontotemporal Dementia (FTD); but also due to its association with declining cognitive and functional ability and decreased quality of life. For example, the Middelheim Frontality Score (MFS) allows the measurement of frontal features distinguishing FTD from AD patients with sensitivity and specificity of almost 90% (95). As impairment of daily living activities are key features of dementia, they must be evaluated using different scales, such as AD Cooperative Study Activities of Daily Living Scale, Functional Activities Questionnaire (FAQ) and Progressive Deterioration Scale (PDS). Most of these scales include measurement of basic activities involving self-maintenance skill, like eating, dressing, bathing; and instrumental activities, which require the use of complex higher order skills as devices, managing finances and shopping [Reviewed in (93)].

The neuroimaging tools like computed tomography and magnetic resonance imaging are used to exclude secondary causes for dementia, such as tumor, inflammatory disease, including abscess or normal-pressure hydrocephalus; or to support and complement clinical features through the evidence of brain regions atrophy [Reviewed in (96)]. Electroencephalography (EEG) is important to provide evidence for Creutzfeldt-Jakob Disease but can also be used to support differential diagnosis of neurodegenerative dementias like AD, DLB, Vascular Dementia (VaD). EEG diffuse abnormalities points to AD but when diffuse and focal changes are both presence DLB, VaD or AD may be the cause (91).

Further, new neurochemical evaluation of CSF can presently assist clinical diagnosis of dementia and contribute to a more accurate diagnosis. This neurochemical diagnosis can be used in differential diagnosis of dementia in particular to distinguish AD from other type of dementia (such as VaD, FTD, DLB). The neurochemical analysis are important in directing towards the right diagnosis, but all results must be interpreted with caution and always depending on clinical data and other diagnostic techniques, such as neuroimaging and neuropsychological testing (97).

1.3. EPIGENETIC AND ALZHEIMER'S DISEASE

The loss of phenotypic plasticity over time is a definition for aging, which is characterized, at the cellular level, by oxidative stress, disturbed calcium homeostasis, chromosomal instability, impaired DNA repair and accumulation of nuclear and mitochondrial DNA damage (43). All these

features can lead to neuronal aging, neurodegeneration, and cell death in the central nervous system (98).

Neurodegenerative diseases are complex disorders that are characterized by the interplay of many genes in their pathology. These complex disorders are characterized by non-Mendelian characteristics, with more percentage of sporadic etiology cases than familiar ones, incomplete concordance rates for monozygotic twins differential susceptibility between males and females, monoallelic expression of susceptibility genes and parent-of-origin effects (16). Epigenetic alterations can explain all these features and aberrant DNA methylation has been shown to be implicated in the pathophysiology of some neurodegenerative diseases [Reviewed in (99)].

Aging is associated with multiple epigenetic alterations and, since it is the major risk factor for AD, may be the mechanism that establishes the connection between environmental/dietary factors and AD development and progression. The normal cell aging process is also associated with a DNA methylation drift with generally global decrease in genomic 5mC in the brain, as well as hypomethylation in all genomic compartments, such as promoter, exonic, intronic, and intergenic regions (100,101).

1.3.1. DNA methylation and AD

In the pathogenesis of AD both hypermethylation and hypomethylation can occur simultaneously in different genes contributing to AD progression (98). AD brains show elevated levels of S-adenosylhomocysteine, a potential inhibitor of methyltransferases that is inversely correlated with patient cognition (102). The promoter CpGs from AD-associated genes, such as *APP*, *PSEN1* and *BACE1* have been reported to be hypomethylated which lead to their abnormal upregulation and the excessive accumulation of A β peptide. Promoters of other genes like *ApoE* and methylenetetrahydrofolate reductase of AD brains cortex showed hypermethylation patterns (101,103).

The frequent methylation of some cytosines in *APP* promoter region in patients with age below 70 years, and the opposite (demethylation) in patients with age above 70 years, supports that model, since the demethylation of APP promoter region can result in an increased APP producing and processing, contributing to AD progression (104). A recent study points to the importance DNMT3a2 as a potential drug target for enhancing or restoring cognitive function due to its interplay in long-term memories and the fact that reduced levels of DNMT3a2 in hippocampus of aged mice models are correlated with cognitive decline through aging (105).

The methylation analysis of *PSEN1*, *ApoE*, Metilenotetrahidrofolato redutase (*MTHFR*) and *DNMT1* genes, the last two involved in methylation homeostasis, pointed to an interindividual epigenetic variability both in post-mortem brain and lymphocytes of AD patients, which may contribute to predisposition to late-onset AD (101). Another study of promoter methylation in peripheral blood genomic DNA, revealed hypermethylation of human telomerase reverse transcriptase (*HTERT*) in AD patients when compared with age matched controls. This gene encodes mRNA that is a component of telomerase and is activated by DNA methylation, in contrast with the normal silencing effect of this epigenetic modification (106).

From a genome-wide perspective, some studies reported decreased DNA methylation in AD, compared with age matched healthy control, in cortical neurons and glia, through immunoreactivity of several markers of DNA methylation. However, no changes in methylation were observed in cerebellum, an area that is not affected in AD patients (107). The same results were also obtained in a study of monozygotic twins discordant for AD and APP-overexpressing transgenic mice (108,109).

1.3.1.1. DNA methylation as a potential biomarker candidate

Biomarkers can be defined as biological molecules in body fluids or tissues that are quantitatively measured and evaluated as indicators of normal biological processes, pathogenesis, or pharmacologic response to therapeutic intervention (110). DNA methylation can easily be detected in a variety of samples, such as tissue and body fluids like peripheral blood and plasma, even in small amounts (111). Aberrant DNA methylation is a well-recognized hallmark of many complex diseases such as heart disease, diabetes, neurological disorders and cancer (35). Global methylation in peripheral blood leukocytes significantly differed between healthy controls and patients with pancreatic cancer, breast cancer, bladder cancer and colorectal adenoma (112–115).

As neurodegenerative disorders have many non-mendelian features, DNA methylation and other epigenetic mechanisms may contribute to the disease pathology and have been extensively studied in order to explain their etiology. Global hypomethylation and hyper and hypomethylation of disease-related genes was detected in postmortem brain tissue of AD patients (104,107,116). Furthermore alterations in DNA methylation levels of several neurodegenerative disorders in peripheral blood cells had also been identified (Table 1).

Table 1 - DNA methylation alterations in peripheral blood cells in neurodegenerative disorders.

Neurodegenerative disorders	Studied Region/gene	DNA methylation alteration	References
Alzheimer Disease	<i>ApoE; MTHFR; HTERT</i>	Hypermethylation	(101,106)
Parkinson Disease	Subtelomeric regions of short telomeres	Hypomethylated subtelomeres	(117)
Multiple Sclerosis	<i>CDKN2B</i>	Hypermethylation	(118)
	<i>MYF3</i> and <i>RB1</i>	Hypomethylation	

DNA methylation has still several limitations that need to be overcome. The clinical use of DNA methylation in peripheral blood leukocytes and whole blood is uncertain as they might not reflect the methylation of target tissues. This limitation is especially important in neurological disorders due to the fact that it is impossible to evaluate the methylation levels in non-postmortem brain samples. Furthermore, DNA methylation analysis techniques don't allow the distinction between 5-mC and 5-hmC, 5-formylcytosine (5-fC), and 5-carboxylcytosine (5-caC); and are unable to differentiate heterogeneous methylation patterns in different cells present within samples (119).

1.3.2. Epigenetic as a potential therapeutic target

Since the discovery of epigenetics, many drugs proved to be capable of reverting abnormal epigenetic changes in particular in cancer and mental disorders. The drugs used can be divided into two classes: DNA methylation inhibitors and HDAC inhibitors (HDACis) (120).

Histone post-translational acetylation is intimately related to gene expression and, therefore, due to histone deacetylation, HDAC action leads to suppression of critical genes in cancer [Reviewed in (121,122)]. Owing to this fact, HDACis were also considered potential targets for mental pathologies and several studies have been carried out with this purpose (123).

Chromatin acetylation plays a role in memory formation (124) and HDACis proved to improve memory and induce dendritic formation, in transgenic mouse model of neurodegeneration (125). These results point to a potential use of HDACis in treating neurodegeneration and memory loss; however, few data regarding the effects of HDACis in brain is available and, despite that, specific gene targets and function in neurodegenerative disorders are still to be revealed (24).

The histone methyltransferase (HMTase) and histone demethylases inhibitors are new groups of drugs that are being developed that may be of therapeutic value. HMTase inhibitors could be used to activate silenced genes but their effects in humans are still to be determined. Alternatively, methylation in different histones and different residues can lead either to gene expression or silencing, for example, H3K9Me2 is related to gene silencing and H3K4Me2 with gene activators; being the state of histone methylation a balance between methylation and demethylation (24,126).

Potentially, DNA methylation can also be a therapeutic target that could allow the change of pathological gene expression. However, a few issues need to be taken into account: it is necessary to understand the methylation patterns in the disease, the complexity of the DNA methylation machinery and the interactions of this machinery with other important processes of the cell (24).

Recently Food and Drug Administration approved DNA methylation inhibitors (5-azacytidine (5-aza) and its analogue 5-deoxycytidine), whose application thus far is restricted to myelodysplastic syndromes (127,128). Besides these two compounds, another DNA methylation inhibitor (Zebularine) has the same mode of action but is chemically more stable and orally bioavailable (129). The mechanism of action of these compounds is based on the inability of DNMT to break the covalent bond to 5'-aza-cytosine. After entering the cell these compounds are phosphorylated to triphosphate nucleotide and incorporate into DNA during DNA replication, resulting in a new strand without methylation, but the template strand with the same methylation pattern [Reviewed in (130)]. Nevertheless, since brain has little mitotic activity the use of these compounds to prevent methylation effects is limited. Furthermore, a study, using these DNA methylation inhibitors, show that long term potential was blocked and was not able to prove with confidence any interaction with DNMT1 (131).

A study using 5-aza in peripheral leucocytes revealed that AD patients lost DNA methylation levels compared with normal and age matched controls, pointing to a deregulation of this process in AD patients (132). Another study, using *in vitro* models, reported that HDACs largely increase H3 and H4 hyperacetylation and the up-regulation of cytotoxic genes, pointing to a histone acetyltransferases inhibitor therapeutic potential in AD (133). This evidence is supported by the decreased risk of developing AD in people consuming large curcumin, a HAT inhibitor that interfere with SPs (134–136).

Therefore, if we think a therapeutic perspective for neuropathologies, there is a need to discover compounds that can affect DNA methylation but independently of the need of DNA

replication, without cell toxicity and able to inhibit directly DNA methyltransferases action. Several compounds have been proposed but they are still in study (137,138) [Reviewed in (130)].

2. Aims of the study

DNA methylation is the major studied epigenetic mechanism and consists in the addition of a methyl group to 5' carbon position of the cytosine ring. In mammals, DNA methylation occurs in CpG dinucleotide that can belong to CpG Islands or CpG Island shores. Methylation of promoter gene regions are directly correlated with gene silencing, which can allow the development of certain diseases as important genes are not expressed due to its promoter methylation. Likewise hypomethylation profiles can also be translated into gene expression alterations. Aging is the major risk factor for AD, and also the process underlying many of the epigenetic alterations.

Detection of global or gene-specific methylation changes can constitute important biomarkers in neurodegenerative disorders, and has also been focus of attention in AD. Furthermore, its evaluation using DNA extracted from body fluids, such as whole blood, constitute a non-invasive method, and, therefore, can allow easier and routine biomarker assessment.

The main goal of this study was to evaluate global or gene-specific methylation changes between possible AD patients and age- and sex-matched controls, therefore the specific aims of this thesis were to:

- (1) Quantify the DNA global methylation levels in possible Alzheimer Disease (AD) patients and compare them with age- and sex-matched healthy controls in a Portuguese pilot study;
- (2) Evaluate gene-specific methylation profiles of AD-related genes, namely APP and *ApoE*, by Combined Bisulfite Restriction Analysis (COBRA);
- (3) Set up the Methylation Sensitive – High Resolution Melting (MS-HRM) conditions to evaluate AD-related gene sequences through melt curve analysis;
- (4) Evaluate methylation profiles of the AD-related genes by Bisulfite Direct Sequencing.

3. Materials and Methods

3.1. SAMPLE CHARACTERIZATION

Inclusion criteria for the study group were: age ranging between 50-90 years, resident in the Aveiro region, with complaints including objective memory impairment or other cognitive symptoms. The exclusion criteria were if individuals undergoing chemotherapy or radiotherapy, psychiatric illness such as bipolar disorder and schizophrenia, and the use of illicit drugs.

The cognitive evaluation of individuals was carried out at several Centers for Primary Health Care in the Aveiro region. The project was approved by the ethics committee of the Regional Health Center - Coimbra, protocol number 012 804 of April 4, 2012.

The Clinical Dementia Rating scale (CDR) (139,140) the Mini-Mental State Examination (MMSE) (141), and the Geriatric Depression Scale (GDS) (142,143) were the cognitive testes applied to the study group. The CDR scale: 0 indicates normal function; 0.5 indicates a transition level (termed questionable dementia); 1.0 indicates significant cognitive function loss (almost always a clear correlation with dementia); 2.0 indicates loss of moderate cognitive function; and 3.0 indicates severe loss. For this study cognitive dysfunction was considered when $CDR \geq 0.5$. The MMSE test allows patient stratification according to the education level: cutoff of 22 for 0-2 years scholarship; 24 for 3-6 years; and 27 for more than 7 years. Additionally, clinical routine questions were included to address other possible neurological pathologies. All depressed individuals were excluded using the GDS scale. This Scale (142,143) consists of 15 questions, in order to survey suggestive symptoms suggestive of depression, in which individuals with 0-5 positive questions were considered normal.

According to the cognitive evaluation, individuals were subdivided in 2 groups: the age- and sex-matched control group (negative for the 3 tests) and the possible AD group (positive for CDR and MMSE scales, negative for GDS).

This study included, 9 possible AD patients and 7 aged- and sex-matched controls (matched as much as possible) from which 2 age- and sex-matched controls and 2 possible AD patients are male. Along with these samples, 1 internal positive control (IPC), which had been diagnosed as AD based on the neurochemical assay of the biomarker triplet ($A\beta$, total Tau and phospho-tau), was also used and the methylation levels evaluated as for the other samples. The mean age for controls is 72 years old and for possible AD patients is 73 years old.

3.2. GENOMIC DNA EXTRACTION

Genomic DNA from samples was extracted using QIAamp DNA Blood Mini Kit (QIAGEN), using 200µl of whole blood from each sample (Figure 7), according to manufactures instructions. The whole blood was added to 20µl of QIAGEN Protease to degrade proteins. In order to guarantee genomic DNA without RNA contamination, 4µl of RNase A (100 mg/ml) was added afterwards. To ensure efficient cell lysis, 200µl of Buffer AL was added to the microcentrifuge tube and mixed, by pulse-vortexing, followed by incubation at 56°C for 15 min.

After centrifugation, 200µl of ethanol (96-100%) were added. The total mixture was applied to QIAamp Mini spin column and centrifuged at 8000rpm for 1 min, allowing the genomic DNA to be retained in silica membrane.

Two wash steps were then performed using Buffer AW1 and Buffer AW2 wash solutions. In the first wash step, 500µl of Buffer AW1 were added to spin columns and centrifuged at 8000 rpm for 1 min. Next, 500µl of Buffer AW2 were also added to spin columns, followed by centrifugation at 14000rpm during 3 min. In order to remove all residues of ethanol and other solutions that may interfere with downstream analysis, an additional centrifugation was performed at 14000 rpm during 1 min.

Finally, the genomic DNA was eluted with Buffer AE, in a total elution volume of 80µl. The quantification and purity of genomic DNA was carried out using NanoDrop Spectrophotometer ND-1000 (Thermo Scientific) and the integrity was visualized by 1% agarose gel electrophoresis.

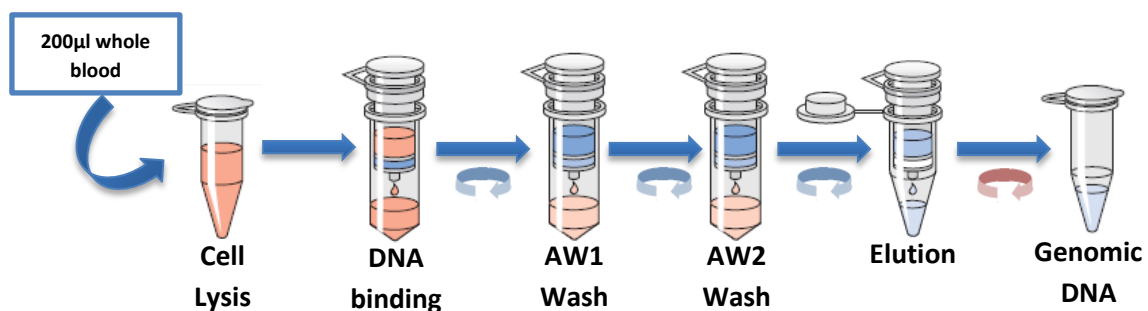


Figure 7 – General steps for pure genomic DNA extraction from whole blood. Blue circular arrow – centrifugation at 8000 rpm; Red circular arrow – centrifugation at 14000rpm. Adapted from QIAamp DNA Blood Mini Kit manual.

3.3. GLOBAL METHYLATION ANALYSIS

For global methylation analysis, Abnova Methylated Quantification Kit (colorimetric) was used which is an enzyme-linked immuno sorbent assay (ELISA) format (Figure 8). For quantification through standard curve, DNA methylated (ME4) control provided in the kit was used to generate five different standard DNA methylation concentrations by dilution in TE 1x buffer as following: 0; 0,5; 1; 2; 5; and 10 ng/ μ l. Unmethylated (ME3) control was used as a negative control.

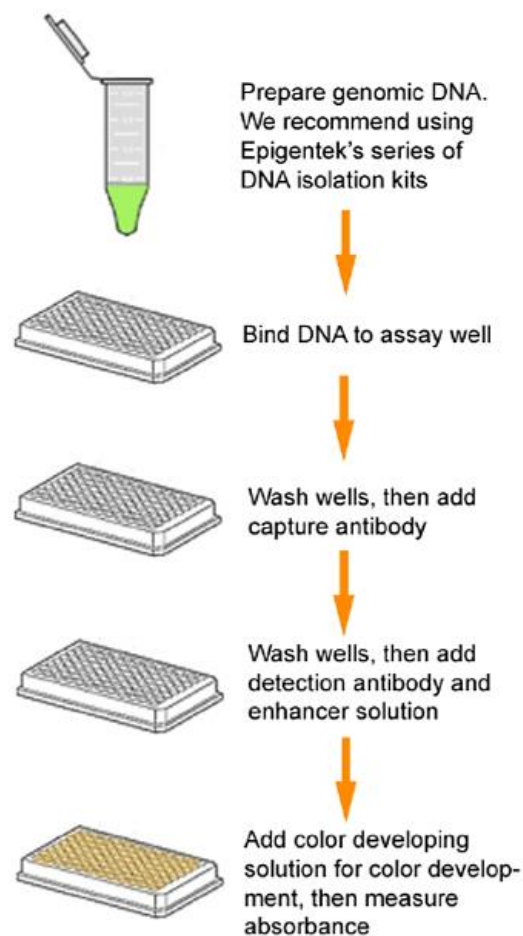


Figure 8 - Schematic representation of the Methylated DNA Quantification by ELISA. Initially DNA is bound to plate well and then capture using antibodies that recognize methylated cytosines. In order to quantify methylated DNA, substrate is added and optical density measured. Extracted from Abnova Methylated Quantification Kit.

After the standard curve preparation, 80 μ l of Binding Solution (ME2) was added to each well, followed by samples and standards. For each control 1 μ l was used. For samples the amount of genomic DNA input was 200ng, previously determined based on NanoDrop Spectrophotometer ND-1000 (Thermo Scientific) quantification, ranging in a volume between 1 μ l and 8 μ l. All samples

and standards were run in duplicates. The plate was incubated at 37°C during 90 min, followed by three washes with ME1 1x Wash Buffer.

Afterwards, the capture of methylated DNA was performed in three steps. First, 50µl of capture antibody (ME5) was introduced in each well and incubated at room temperature for 1h, to enable the recognition of methylated DNA. Secondly, the samples and controls were incubated with 50µl of detection antibody (ME6) at room temperature during 30 min. The last step was incubation at room temperature for another 30 min, with 50µl of enhancer solution (ME7) to increase the signal's assay. Between all three steps, the wells were washed four times with ME1 1x Wash Buffer.

Finally, the signal was generated by adding the developer solution (ME8) and the enzymatic reaction was stopped (ME9) as soon as the most concentrated standard exhibit blue. Absorbance was measure at 450nm using TECAN infinite M200. The amount and percentages of methylated DNA were calculated according to manufacturer instructions, as following:.

$$5 - \text{mC (ng)} = \frac{\text{Sample OD} - \text{ME3 OD}}{\text{Slope} \times 2}$$

$$5 - \text{mC \%} = \frac{5 - \text{mC Amount (ng)}}{S} \times 100\%$$

Figure 9 - Calculation of DNA methylation (5-mC) percentages. In order to determine the amount of methylated DNA, the optical density (OD) of negative control (ME3) is subtracted to OD of samples and divided by standard curve slope. However, as the methylated DNA control only has 50% of methylated cytosines, it was necessary to normalize samples dividing by 2. Then, the amount of methylated DNA is divided through the amount of DNA input followed by the multiplication by 100 to reach DNA methylation percentages. Extracted from Abnova Methylated Quantification Kit.

3.4. BISULFITE DNA MODIFICATION

Bisulfite conversion is a wide method to evaluate DNA methylation. Chemically, sodium bisulfite cytosine desamination is completed through three reactions (Figure 10). The first is sulphonation, which consists in the addition of bisulfite to the 5-6 double bond of cytosine, followed by hydrolytic deamination resulting in uracil-bisulfite derivate. The final step is alkali desulphonation that consists in the removal of sulphonate group by alkali treatment, originating uracil nucleotide. As methylated cytosine has a methyl group in position 5, they are protected

against bisulfite mediated deamination. In order to these reactions to occur, the DNA must be single stranded and, therefore, a correct denaturation step is crucial. After PCR, methylated cytosines remain intact and non-methylated cytosines appear in DNA fragment as thymines (144).

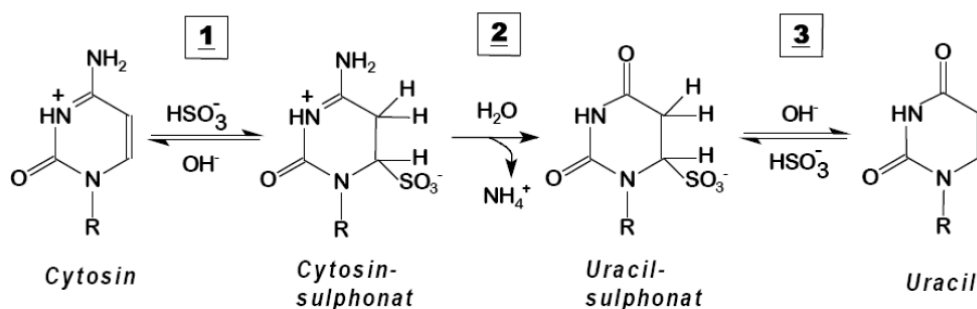


Figure 10 - Bisulfite conversion reactions. The three steps, sulphonation (1), hydrolytic deamination (2), alkali desulphonation (3) lead to non-methylated cytosine desaminations and, subsequent, conversion into uracil. Extracted from (145)

The bisulfite conversion was carried out using EZ DNA Methylation-Gold Kit (Zymo Research). For all samples 1 μg of genomic DNA, calculated based on quantification of NanoDrop, was modified according with manufacture indications. A maximum of 40 μl of DNA volume was used, and samples normalized for the volume using nuclease free water. The CT Modification Reagent was then added (110 μl) and samples were submitted to the conditions present in Table 2 using MyCyclerTM Thermal Cycler (BioRad).

Table 2 - Bisulfite conversion conditions.

Step	Temperature ($^{\circ}\text{C}$)	Duration
1	98	10 min
2	64	2.5 hours
3	4	hold

Once bisulfite conversion finished the bisulfite modified DNA (bDNA) was bound to spin columns by mixing samples with 600 μl of M-Binding Buffer, followed by centrifugation at 12000xg for 30 sec. Before the desulphonation step, the bDNA was washed using M-Wash Buffer and centrifuged for 30 sec. In order to remove residues of bisulfite conversion reagent, 200 μl of M-Desulphonation Buffer was added to the columns and incubated for 20 min at room temperature. Next, the columns were centrifuged and two wash steps performed as mentioned above to ensure the complete removal of PCR inhibitors, like ethanol or even any remaining of the

desulphonation solution. Finally, the bDNA was eluted using nuclease free water. To increase the elution efficiency, before centrifugation at 12000 xg for 30 sec, the columns were incubated for 5 minutes at room temperature. After bisulfite modification, the bDNA is a single strand molecule with both DNA and RNA features and thereby it is not accurately quantified by spectrometry. The bDNA was stored at -80°C.

3.5. SELECTION OF METHYLATED GENE REGION

The sequence from *APP* and *ApoE* was extracted from UCSC Genome Bioinformatics, with 4000 bases upstream gene region, and blasted in the NCBI to verify its identity. Information regarding the *APP* and *ApoE* sequences used is present in Table 3. For each gene, the translation start codon was assessed through NCBI search and the transcription start site (TSS) annotated base on research articles (146,147).

Table 3 – Information about genes sequences according to UCSC Genome Bioinformatics.

Gene	Reference Sequence	Chromosome	Chromosome position
<i>ApoE</i>	NM_000041	19	45406039-45412650
<i>APP</i>	NM_001204301	21	27252861-27546138

The gene sequences were introduced in CpG Island Searcher (<http://cpgislands.usc.edu/>), in order to find CGIs. The CGIs were also confirmed during primer design, using the Methyl Primer Express v1.0 (Applied Biosystems) software.

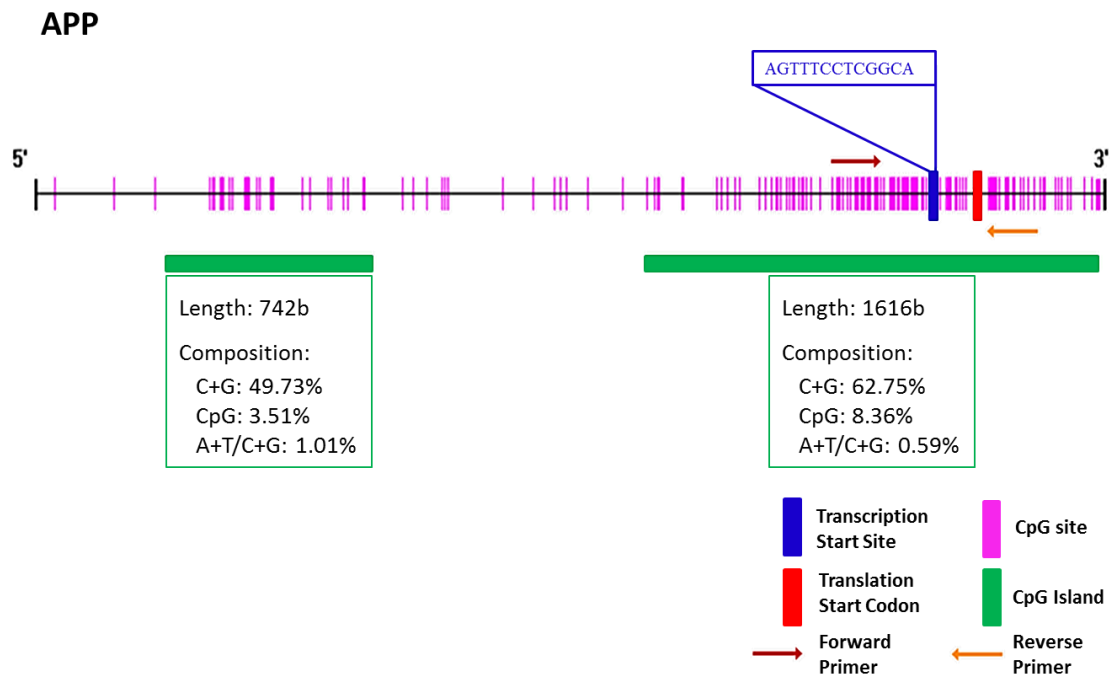


Figure 11 - CpG islands present in *APP* promoter region sequence. The selected and amplified region is localized between primers. The major transcription start site (TSS) was annotated based on Salbaum, 1988 (146).

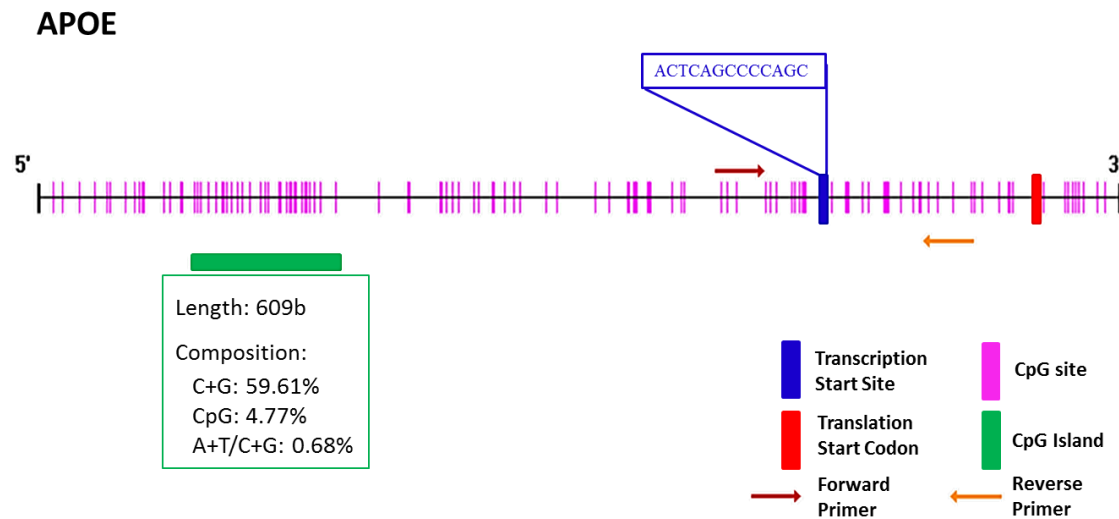


Figure 12 – The *ApoE* promoter sequence exhibit only one CpG Island upstream transcriptional start site (TSS). The selected and amplified region is localized between primers. The TSS was annotated based on Paik, 1985 (147).

3.6. PRIMER DESIGN

The selected regions for *APP* and *ApoE* genes were selected according to TSS region and included the positions between -256 and +178 for *APP* and between the -120 and +283 for the

ApoE gene. The *APP* and *ApoE* selected sequences were introduced in Methyl Primer Express V1.0, a primer design software. This software is specific in designing primers for methylation analysis using bisulfite conversion, as it converts automatically genomic sequence and show the best primer pairs for bisulfite modified DNA. For *APP* 3 sets of primers were designed; one for Combine Bisulfite Restriction Analysis (COBRA) and two for Methylation Sensitive - High Resolution Melting (MS-HRM), and for *ApoE* only one set of primers were designed. In MS-HRM, *APP* promoter region was set to two fragments of approximately 250bp in order to provide better analysis due to high CpG density. The primers used in each approach will be identified in the corresponding sections.

The sets of primers designed were tested for self-complementary and hetero dimerization using AutoDimer V1. All sets of primers exhibit interactions below score number 4, despite the acceptable score for multiplex PCR being 7. The primer sets were also tested in other software such as Thermo Scientific Multiple Primer Analyzer (available in <http://www.thermoscientificbio.com/webtools/multipleprimer/>), exhibiting low levels of interactions. Temperature melting of primers was also estimated using IDT OligoAnalyzer 3.1 (available in <http://eu.idtdna.com/analyzer/Applications/OligoAnalyzer/>).

3.7. COMBINE BISULFITE RESTRICTION ANALYSIS

The COBRA consists in amplification of a bisulfite modified genomic sequence using specific primers, followed by restriction analysis with enzymes that recognize methylation sites. After bisulfite treatment, only the non-methylated cytosines convert to uracil and, therefore, the recognition site for restriction enzymes of methylated cytosines remain the same. After PCR reaction, enzymatic restriction digestion products were run in an agarose gel to chase for the methylation pattern in each sample.

3.7.1. Amplification of *APP* and *ApoE* sequences by PCR

For this method the set of primers were designed as described in section 3.6. Table 4 shows the primers used for *APP* and *ApoE* Genes.

Table 4 - Sets of primers used for *ApoE* and *APP* amplification for COBRA.

Gene	Primer sequence	Annealing Temperature	PCR product length
<i>ApoE</i>	Fw: 5' GGGTAGGGGGGAGAATAGTTTAT 3'	59°C	403bp
	Rv: 5' CTTACATCCCAATCCAACACTACT 3'		
<i>APP</i>	Fw: 5' TGGTTTTAGATTTTTTTTTTTTATTGT 3'	56°C	434bp
	Rv: 5' CCAACAAAAACAATACCAAACC 3'		

The PCR reactions were done in a final volume of 25µl as described in Table 5.

Table 5 – PCR amplification reaction composition.

Components	Volume/reaction (µl)
bDNA (≈20ng/µL)	5
Master Mix	12.5
Primer Fw (5µM)	1.5
Primer Rv (5µM)	1.5
Nuclease free water	4.5
Total	25

The PCR program, described in Table 6 and Table 7, was performed in MyCycler™ Thermal Cycler (BioRad).

Table 6 - PCR cycling conditions for *APP* gene amplification using Maxima HotStart.

Number of cycles	Step	Temperature (°C)	Duration
1	Initial denaturation	95	10 min
45	Denaturation	95	30 sec
	Annealing	56	30 sec
	Extension	72	1 min
1	Final extension	72	7 min

Table 7 - PCR cycling conditions for *ApoE* gene amplification using Kappa Uracil+.

Number of cycles	Step	Temperature (°C)	Duration
1	Initial denaturation	95	5 min
40	Denaturation	98	20 sec
	Annealing	59	15 sec
	Extension	72	1 min
1	Final extension	72	1 min

3.7.1.1. Agarose gel electrophoresis

Agarose gel electrophoresis is the method of choice for separating DNA fragments from different sizes. The phosphate groups charge negatively the DNA molecule allowing its migration to the positive terminal, when subjected to an electrical field. Since DNA has uniform mass/charge ratio, fragments from different sizes can be separated using the appropriate agarose percentage gel. The larger DNA fragments have less migration rate than small size DNA fragments. Furthermore, the migration rate also depends on the agarose concentration and type, the running buffer, the DNA conformation and the voltage applied (148).

To confirm the presence of the expected DNA fragment, PCR products were visualized using 2% agarose gels prepared in 1x TAE Buffer. After boiling, the gel was cooled down to 60°C and then GreenSafe (NZYTech) was added to a final concentration of 0.025µl/ml and the solution poured into the gel tray to allow proper polymerization. Samples were prepared by adding glycerol in the ratio 1:6, to increase sample density. The DNA ladder 1kb plus (Invitrogen) was used. The gel was run at 90V for about 40 minutes. Finally, the gels were visualized under UV light in Gel Doc XR System (Bio-Rad).

3.7.2. Restriction Enzyme Selection and Digestion

The selection of the restriction enzyme was carried out using a simulator present in the *In silico simulation of molecular biology experiments* site (<http://insilico.ehu.es/>). After introducing the methylated sequence, the online tool generates an unmethylated sequence and tests all commercial available enzymes. The enzyme was chosen based on the cleavage sites in the methylated sequence, and consequently on the fragment pattern complexity obtained.

The enzymes chosen were **HhaI** (recognition site: GCG'C) (Thermo Scientific) and **SsiI** (recognition site: G'CGG) (Thermo Scientific) to analyze *APP* (Figure 13) and *ApoE* (Figure 14),

respectively. The HhaI has seven potential cut sites in *APP* sequence, originating a maximum of eight fragments. On the other hand, SsiI has three potential cleavage points given rise to a maximum of four fragments, if all CpG exhibit methylation.

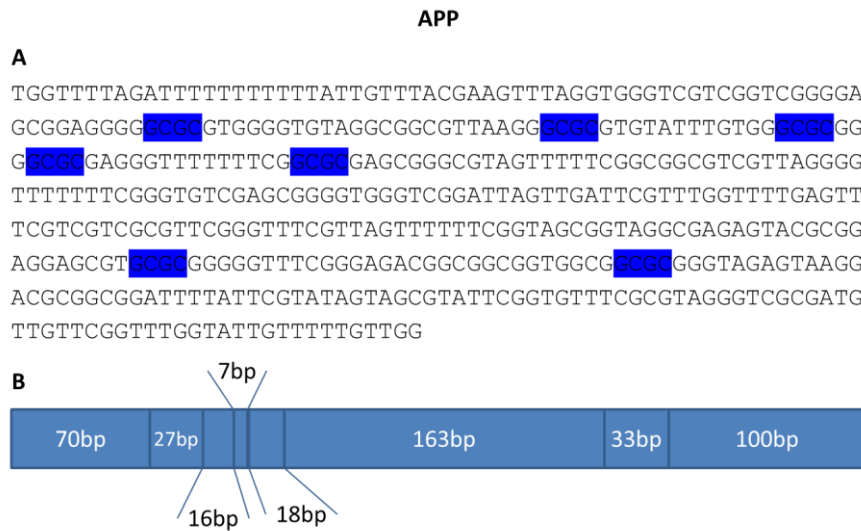


Figure 13 – Restriction recognition sites of HhaI in amplified *APP* sequence (A) and fragments originated from methylated DNA digestion (B).

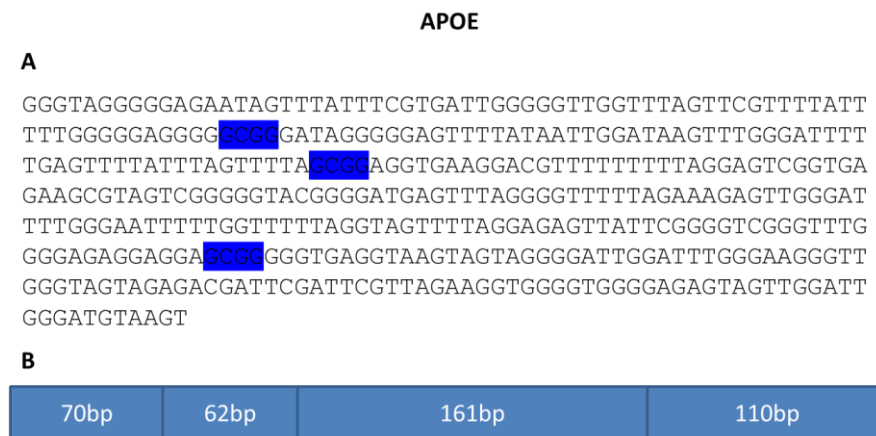


Figure 14 – Restriction recognition sites of SsiI in amplified *ApoE* sequence (A) and fragments originated from methylated DNA digestion (B).

The enzymatic digestion was performed at 37°C overnight (~16 hours), as described in Table 8.

Table 8 - Enzymatic restriction mixture components.

Components	<i>APP</i>	<i>ApoE</i>
	Volume/reaction (μl)	Volume/reaction (μl)
PCR product	17	17
HhaI (10U/μl)	1	-
SsiI (10U/μl)	-	1
Buffer Tango	2.5	-
Buffer O	-	2.5
Nuclease free water	4.5	4.5
Total	25	25

The resulting restriction fragments were run analyzed in 3% agarose gel as described in section 3.7.1.1, using instead of TAE 1x, SGTB buffer 1x as it allows better results in separation of small DNA size fragments that may arise from enzymatic digestion (149). Gel was run at 200V for approximately 25min and visualized under UV light in Gel Doc XR System (Bio-Rad).

Methylated and unmethylated DNA controls were used and treated exactly as the samples. The DNA of both controls came from HCT116 DKO cell which has genetic knockouts for DNA methyltransferases DNMT1 and DNMT3b. The DNA extracted from these cells has less than 5% methylation and serves as unmethylated control. For the methylated control, the DNA was subjected to enzymatic methylation using M. SssI methyltransferase. Validation of unmethylated and methylated DNA controls were carried out by the manufacture by amplifying a specific region of the gene BRCA1 with methylated and unmethylated specific primers.

3.8. METHYLATION-SENSITIVE HIGH RESOLUTION MELTING (MS-HRM)

The MS-HRM is a recent technique that allows the DNA methylation quantification in a gene sequence by comparison with methylated and unmethylated standards, using real-time PCR technology. The initial step consists in the amplification of the sequence using primers that amplify regions regardless their methylation state. During the amplification, DNA binding dye intercalate with double strand DNA emitting fluorescence. After the amplification step, PCR products are gradually denatured by increasing the temperature in small increments, resulting in a characteristic melting profile. As the DNA denatures, the dyes are released and fluorescence is lost. According to high amount of C/G or A/T content of the DNA, it can denature at higher or

lower temperatures, respectively. The bDNA molecules differ only in cytosine content, with higher cytosine content having higher melting temperatures and high methylation percentages. Through the comparison of samples melting profile with melting profiles from known methylation standards, the methylation percentage of samples can be determined (150).

To evaluate methylation in the *APP* and *ApoE* genes MS-HRM was used as an alternative approach. In order to achieve better analysis through MS-HRM due to excessive number of CpGs sites, the *APP* gene sequence amplified before, was divided into two small fragments with 223bp and 236bp in length that were amplified using the primers listed in Table 9. On the other hand, as *ApoE* did not contain so many CpG sites, the same primers used in section 3.7.1 were also used.

Table 9 – Primers used in MS-HRM for methylation analysis of *ApoE* and *APP*.

Gene	Primer sequence	Annealing Temperature (°C)	PCR product length (bp)
<i>ApoE</i>	Fw1: 5' GGGTAGGGGGGAGAATAGTTTAT 3'	62	403
	Rv1: 5' CTTACATCCCAATCCAACACTACT 3'		
<i>APP</i>	Fw1: 5' TGGTTTTAGATTTTTTTTTTTTATTGT 3'	61	223
	Rv1: 5' AACCAAACRAATCAACTAATCC 3'		
	Fw2: 5' GGTGGGTYGGATTAGTTGAT 3'	62	236
	Rv2: 5' CCAACAAAACAATACCAAACC 3'		

The methylation percentages can be easily accessed through comparison with a standard curve with defined methylation ratios. The different methylation percentages were prepared by mixing methylation controls from CpGenome™ Human Methylated & Non-Methylated DNA Standard Set (Millipore) in different ratios. To generate the standard curve the methylation percentages used were: 0; 1; 2; 5; 10; 25; 50 and 100. All standards and samples underwent bisulfite modification at the same time and conditions. The PCR reaction was prepared according to Table 10 and all samples, along with standards, were run in duplicates applying the PCR program listed in Table 11, using StepOnePlus Real-Time PCR System (Applied Biosystems).

Table 10 – PCR reaction for real-time amplification.

Components	Volume/reaction (μl)
bDNA (≈20ng/μL)	2
MeltDoctor™ HRM Master Mix	10
Primer Fw (5μM)	1.2
Primer Rv (5μM)	1.2
Nuclease free water	5.6
Total	20

Table 11 – MS-HRM PCR program.

Number of cycles	Step	Temperature (°C)	Duration
1	Initial denaturation	95	10 min
40	Denaturation	95	15 sec
	Annealing/Extension	Primer T _m (see Table 9)	1:30 min
1	Melt curve	95	10 sec
		60	1 min
		60 / 95	-

3.8.1. High Resolution Melting (HRM) analysis

The methylation of samples was evaluated comparing the melt curve pattern of standard, using High Resolution Melt (HRM) Software v3.0.1. Before determining methylation percentages, amplification plots and melt curves of all samples and standards were analyzed to assure PCR specificity.

3.9. DIRECT BISULFITE SEQUENCING

PCR products of *ApoE* gene were generated as detailed in **section 3.7.1**. The purification of PCR products was done using QIAquick PCR Purification Kit (Qiagen), according to manufactures instructions. Buffer PBI was added to PCR products in a ratio of 1:5 and then applied to the spin columns. The columns were then centrifuged at 10000 xg during 1 min. After, Buffer PE was added to the columns and then centrifuged in the same conditions. In order to

obtain PCR products with high levels of purity, another centrifugation step was performed. The elution of DNA from columns was carried out using 30µl of Mili-Q water, incubation 5min at room temperature and then centrifuged at 10000 xg for 1min. The purity and concentration of PCR products was evaluated using NanoDrop Spectrophotometer ND-1000 (Thermo Scientific).

For the sequencing reaction, 3 ng of PCR products was used along with an internal reverse primer (sequence: 5' CCAACTCTTTCTAAAAACCCCT 3'), under PCR conditions present in the Table 12. The DNA was precipitated by adding sodium acetate (3M, pH 5.2) and absolute ethanol in a 1:10 and 2.5:1 ratio, respectively; vortexed and incubated for 15min at room temperature. After, the samples were centrifuged at 14000rpm for 20min. The pellet was then washed with 250µl of 70% ethanol and centrifuged at 14000rpm for 5min. The supernatant was removed and dried at 37°C for approximately 1 hour, and the resuspended in 20µl of formamide.

The samples were applied in ABI PRISM™ Genetic Analyzer 310 (Applied Biosystems) and the results were analyzed using Sequence Scanner 2 (Applied Biosystems) and BiQ Analyzer (available in <http://biq-analyzer.bioinf.mpi-inf.mpg.de/index.php>).

Table 12 - PCR conditions for PCR sequencing reaction.

Number of cycles	Step	Temperature (°C)	Duration
1	Initial denaturation	96	1 min
25	Denaturation	96	30 sec
	Annealing	42	15 sec
	Extension	60	4 min

For qualitative analysis, CpG with 20% or lower were considered unmethylated, and CpG with methylation percentage above it were treated as methylated (partially methylated between 20%-80%; and above 80% considered methylated). On the other hand, for quantitative analysis of CpG sites, the methylation percentages of each were calculated according with the following equation (151):

$$\text{Methylation \%} = \frac{y \text{ value of } G \text{ peak}}{y \text{ value of } G \text{ peak} + y \text{ value of } A \text{ peak}} \times 100$$

4. Results

4.1. GENOMIC DNA EXTRACTION FROM WHOLE BLOOD SAMPLES

Genomic DNA extraction of all samples was carried out as described in section 3.2. Upon extraction, the purity and concentration of DNA samples was determined using a NanoDrop spectrophotometer. Genomic DNA samples exhibited 260/280 ratios between 1,70 and 1,89; and concentrations that ranged from 27,6 ng/μl to 51,5 ng/μl (Table 13). Concentrations were within the expected values, which were 30-60 ng/μl according to the manufacture instructions.

Table 13 - NanoDrop results of samples genomic DNA.

Condition	COD	Age	260/280 Ratio	DNA Concentration (ng/μl)
Age- and Sex-Matched Controls	C1	49	1,89	50,5
	C2	72	1,87	28,6
	C2'	72	1,85	39,2
	C3*	75	1,86	36,4
	C7	78	1,86	51,5
	C8	74	1,81	31,0
	C9	82	1,80	51,5
Possible AD Patients	D1	49	1,78	37,9
	D2*	72	1,86	35,7
	D3	74	1,79	36,1
	D4	74	1,79	48,6
	D5	76	1,88	30,2
	D6	76	1,70	34,4
	D7	80	1,81	52,3
	D8	74	1,84	27,6
	D9	83	1,81	40,2
Internal Positive Control	IPC	78	1,84	46,3

* C3 was the age- and sex-matched control for patients D3-D6. D2 has 2 controls (C2 and C2').

In all samples the DNA did not show signs of degradation and bands intensity were in general proportional to genomic DNA concentration determined (Figure 15). The gDNA yield correlates with the number of white blood cells, which may vary among individuals according to

age, sex and immune system, among other factors, thus explaining the different concentrations obtained.

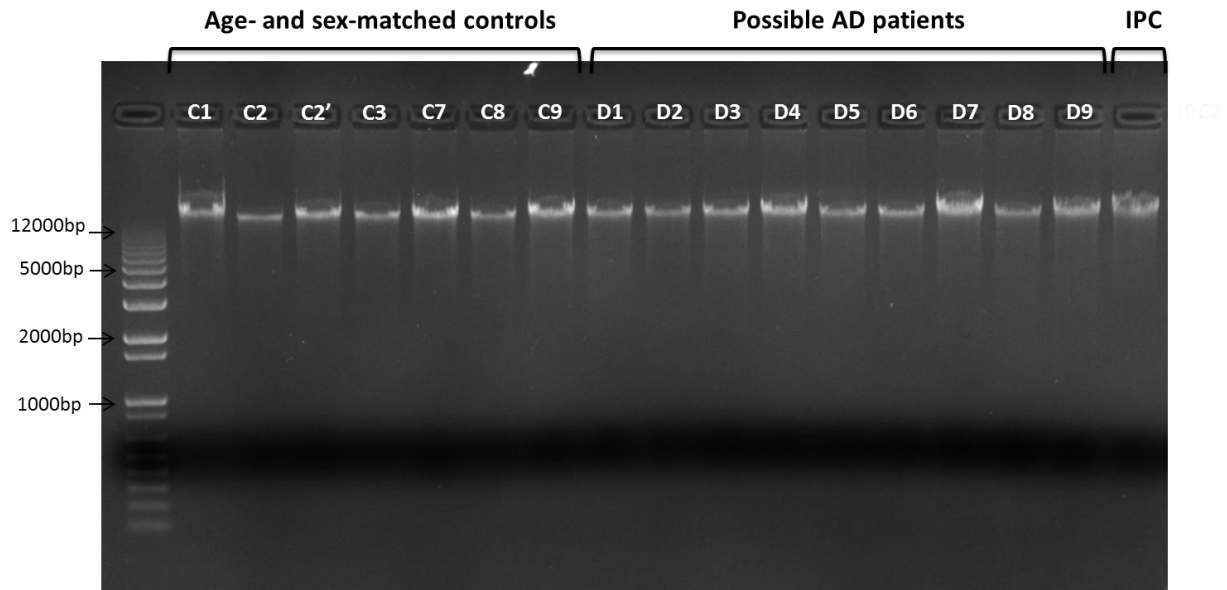


Figure 15 - Genomic DNA agarose gel electrophoresis. Samples were loaded in a 1% agarose gel.

4.2. GLOBAL METHYLATION LEVELS IN AD PATIENTS

The global methylation levels of samples were determined using an ELISA-based assay. As expected the levels of methylation were very low, ranging from 0,3 % to 1,1%. In general, the global methylation levels mean of AD patients were lower when compared to age- and sex-matched controls (0,75% ($\pm 0,29$) vs 0,86% ($\pm 0,29$)) (Figure 16). The only exceptions were the patients D2 and D9. Although no clear correlation could be observed between age and the methylation levels in the study group, these results point to a global hypomethylation in possible AD patients, relatively to age- and sex-matched control individuals.

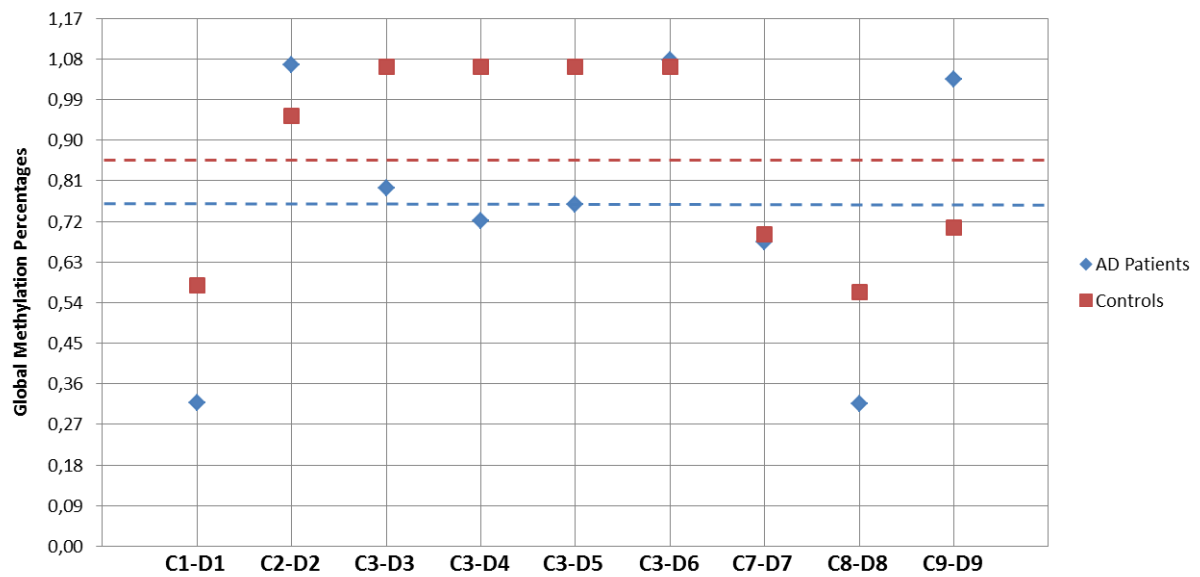


Figure 16 - Dispersion graphic of global methylation percentages of possible AD patients and age- and sex-matched controls. The blue and red dashed lines represent the mean of global methylation levels for possible AD patients and age- and sex-matched controls, respectively. The pairs C8-D8 and C9-D9 are males while the other samples are females. Controls and patients were age- and sex- matched (table 15).

4.3. METHYLATION LEVELS IN AD ASSOCIATED GENES

Different approaches were used to evaluate the methylation of promoter regions in *APP* and *ApoE* genes, the PCR amplification of the region followed by enzyme restriction, the MS-HRM and bisulfite direct sequencing. As methylated and unmethylated strands amplify better at different temperatures, methylated and unmethylated DNA controls were tested to determine the temperature in which both strands amplify at similar proportions. MS-HRM was also optimized using methylated and unmethylated DNA controls. The reaction was considered to be optimized when both methylated and unmethylated strands amplified at equal proportions (optimal PCR conditions were described in M&M section).

4.3.1. Restriction pattern of *APP* and *ApoE* genes in AD patients

To evaluate if the restriction pattern of promoter regions were different among control and disease patients, the DNA was first bisulfite modified and then amplified for the regions of interest. Both genes were successfully amplified and the expected product size of 403bp for *ApoE* and 434bp for *APP* obtained for all samples (Figure 17 and Figure 18).

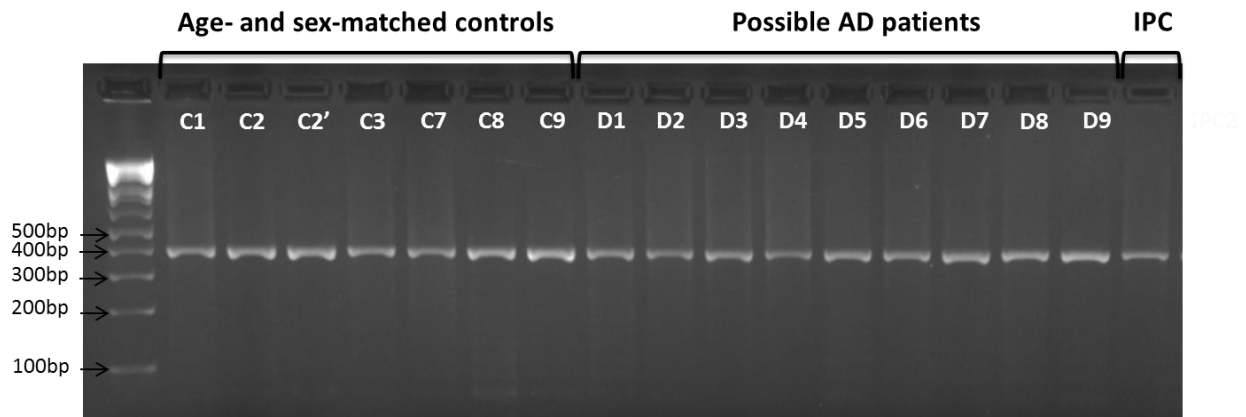


Figure 17 - *ApoE* promoter sequence amplified by PCR. All samples were successfully amplified and the 403bp fragment obtained. Along with the aged- and sex-matched controls, an **IPC** sample was included.

In the case of *APP* gene, two samples (D1 and D2) showed a slightly lower DNA size band than expected, probably due to a problem during the gel preparation or due to excessive loading dyes. Nonetheless both samples, similarly to the others, exhibited the same DNA size after restriction digestion, indicating that the fragment was correctly amplified.

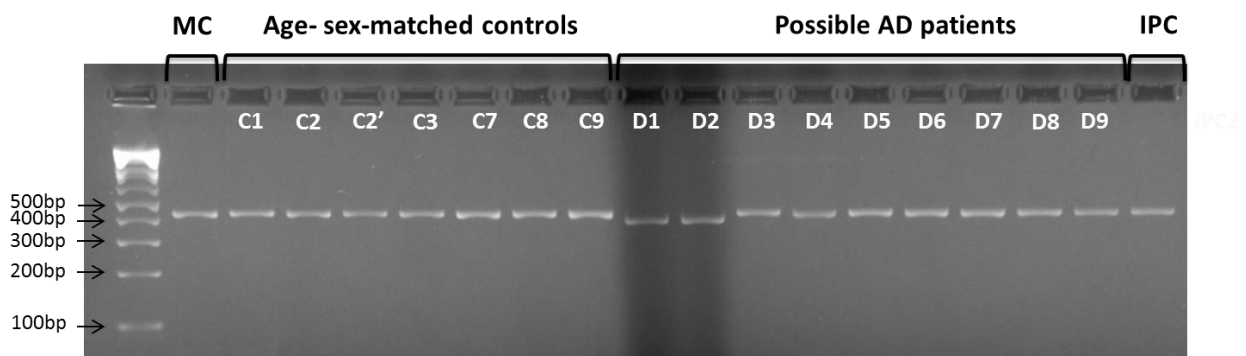


Figure 18 - *APP* promoter sequence amplified by PCR. All samples were successfully amplified and the expected size fragment of 434bp obtained. Along with the aged- and sex-matched controls, an **IPC** and a 100% Methylated DNA Control (**MC**), were included.

Following PCR amplification the resulting fragments were incubated with different restriction enzymes in order to obtain a restriction pattern (COBRA) of samples. The evaluation of the efficiency of the restriction digestion reaction was done by using a methylated DNA control, in which all cleavage sites are methylated. For this control all the expected DNA fragments, after digestion, were visible, both for *ApoE* and *APP* gene as explained in Figure 13 and Figure 14 (section 3.7.2).

Under these conditions no distinct pattern was observed that could differentiate AD patients from age- and sex-matched controls, with both groups exhibiting heterogeneous methylation levels (Figure 19).

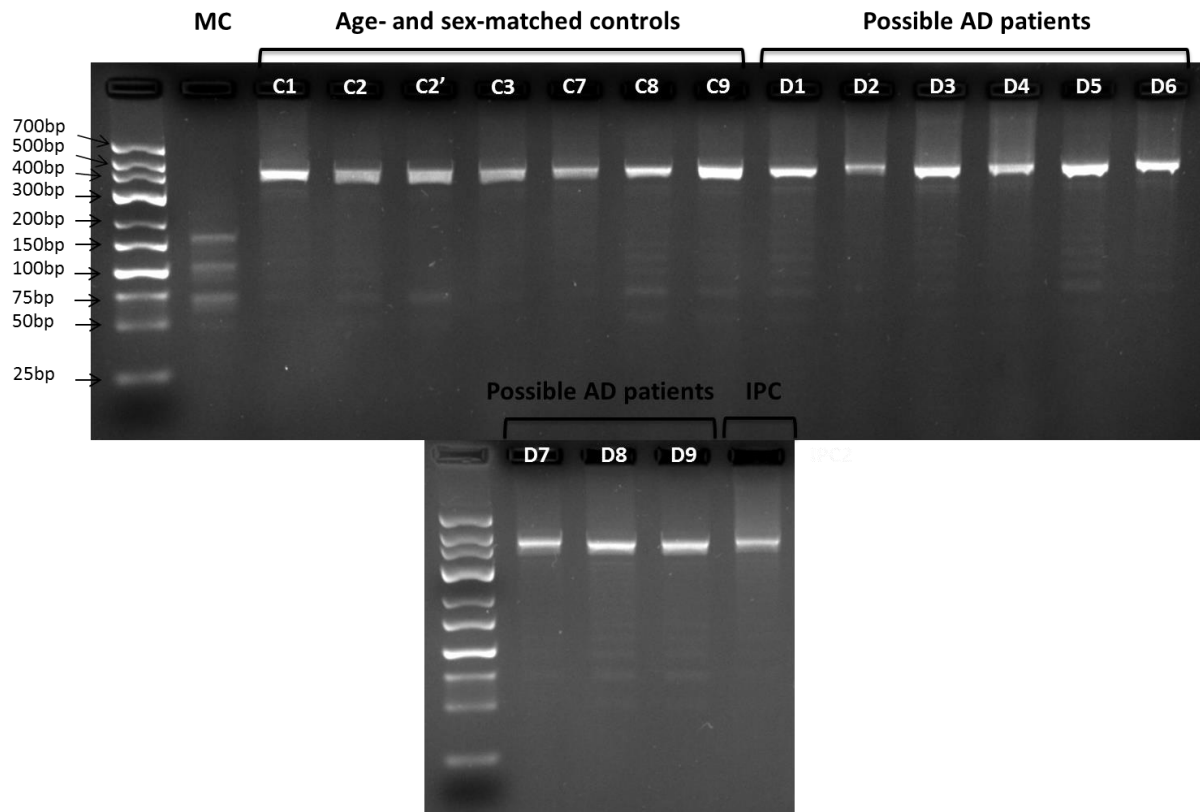


Figure 19 - Electrophoretic analysis of *ApoE* promoter sequence restriction by *SsiI*. All samples exhibited good amplification signals and no distinct pattern could be observed among groups for the region in study. Along with the study group samples, an internal positive control (IPC) and a 100% Methylated DNA Control (MC) were included.

For *APP* gene, no methylation could be observed neither for AD patients nor age- and sex-matched controls, as all fragments have approximately the entire DNA fragment size. The two bands of approximately 70bp and 50bp, present in all samples, correspond to non-specific product since no intermediate bands was seen, suggesting the inexistence of methylation for the *APP* region in study (Figure 20).

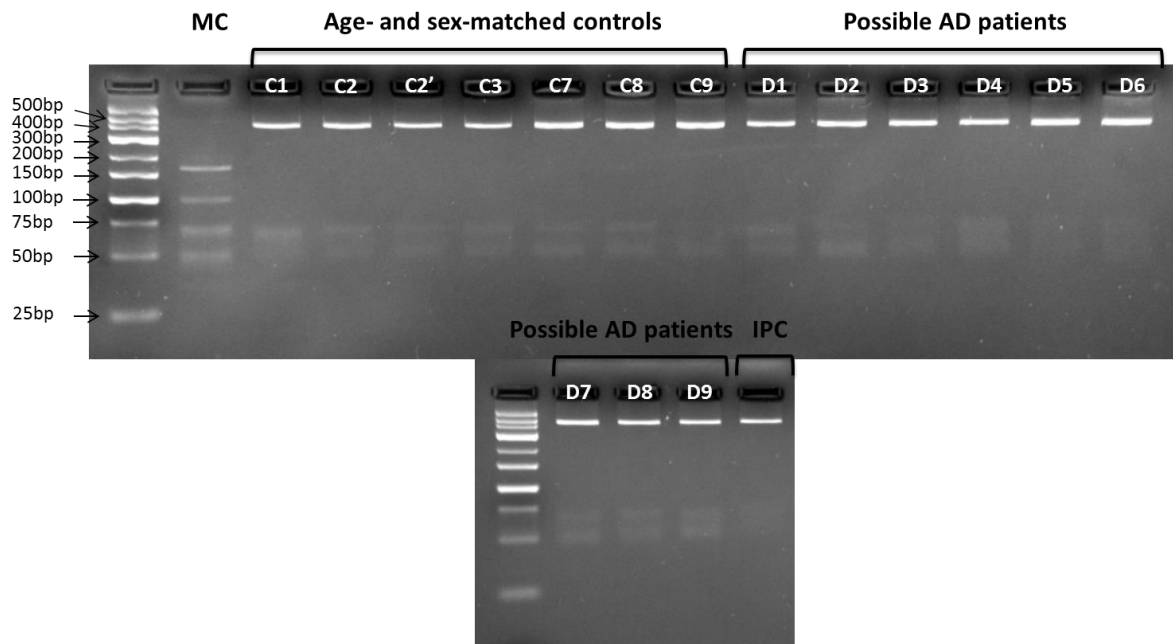


Figure 20 - Electrophoretic analysis of *APP* promoter sequence restriction by *HhaI*. All samples showed a good amplification signals nonetheless no restriction pattern could be observed, indicating the absence of methylation in the enzyme recognition sites of this promoter region. The two bands with lowest size are unspecific products.

4.3.2. Evaluation of *ApoE* and *APP* methylation levels by MS-HRM

Using MS-HRM technique the *ApoE* promoter region was successfully amplified for all cases, nonetheless, and contrary to what was expected both unmethylated and methylated DNA controls exhibited similar methylation levels (verified by sequencing) for this region, therefore it was not possible to prepare standards to determine the precise methylation levels of each sample. Although a quantitative assay was not viable, by comparing the melting curves using HRM software (Figure 21) it was possible to group the samples into two variants (Table 14). However, these two variant groups contained both AD patients and controls, not allowing their distinction, at least for the *ApoE* regions evaluated using this approach.

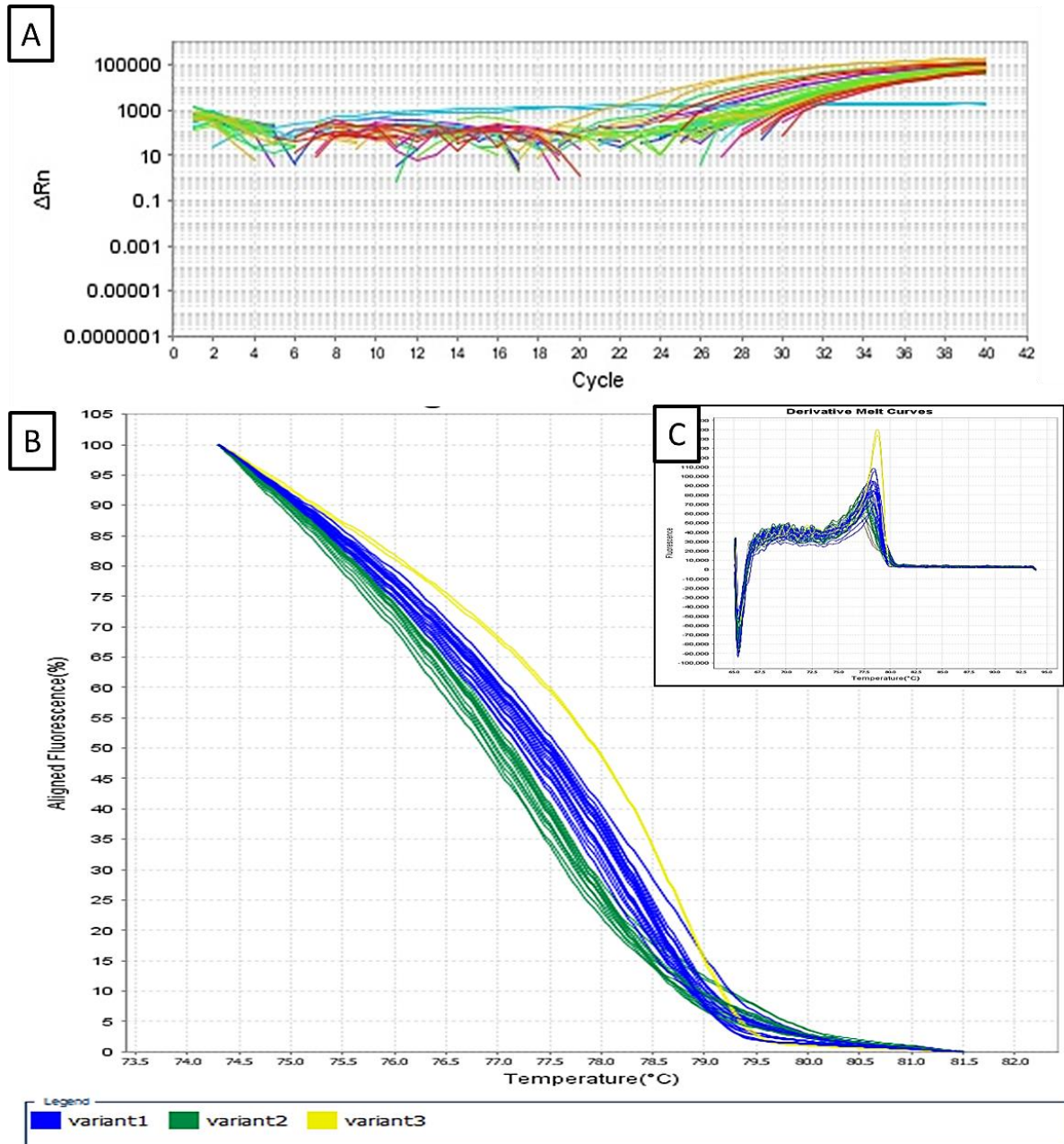


Figure 21 – HRM curve generated by amplification of *ApoE* gene. **A** – Amplification plot for samples and methylation DNA controls with each color corresponding to a sample. **B** – Aligned melt curves between 74,0°C and 81,5°C with samples grouped by variants according with the similar melting behavior.; **C** – Derivative melt curves exhibiting the amplification of only one fragment with low differences melting temperatures due to the presence of a single peak in each sample, controls and DNA methylation control. No distinct profile could be observed with both possible AD patients and age- and sex-matched controls localized in the same variants (detailed in table 14).

As *APP* promoter gene region had many CpG sites, this region was amplified using two different sets of primers and independently PCR conditions, which amplified the region upstream (Figure 22) and downstream (Figure 23) of the TSS. In both cases, the samples showed identical melting profiles indicating similar levels of methylation. Unexpectedly, the unmethylated DNA

control exhibited methylation levels above samples, indicating that for the region in study this control is at least in part methylated, thus not representing a real unmethylated control.

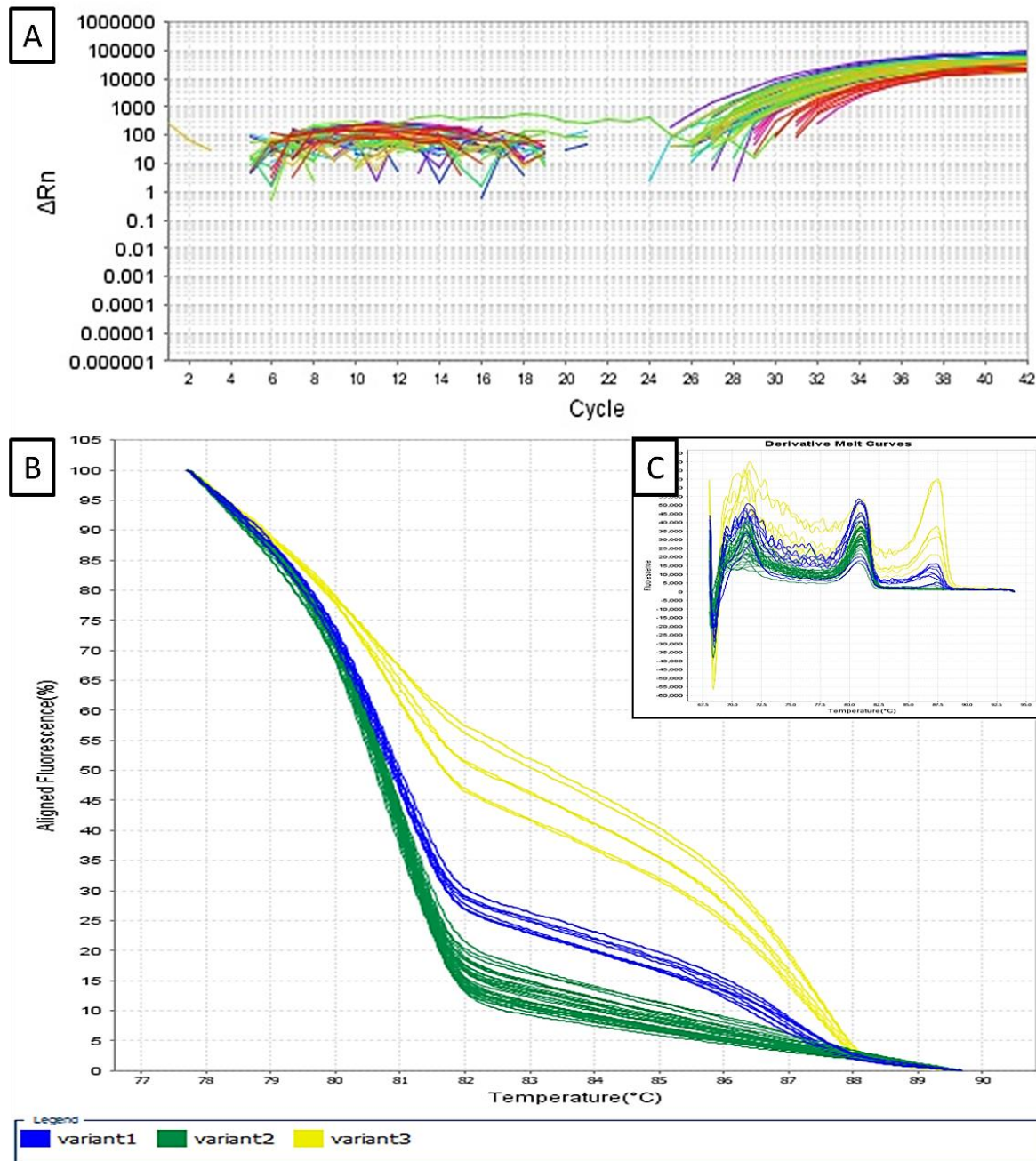


Figure 22 – HRM curve generated by amplification of *APP* region upstream TSS (first primer set). **A** – Amplification plot for samples and methylation DNA controls with each color corresponding to a sample. **B** – Aligned melt curve between 77,9°C and 89,5°C with samples grouped by variants according with the similar melting behavior ; **C** – Derivative melt curves showing two main peaks at 81°C and 87,5°C that correspond to unmethylated and methylated DNA fragment population, respectively. No distinct profile could be observed as both possible AD patients and age- and sex-matched controls were localized in the same variants.(detailed in table 14).

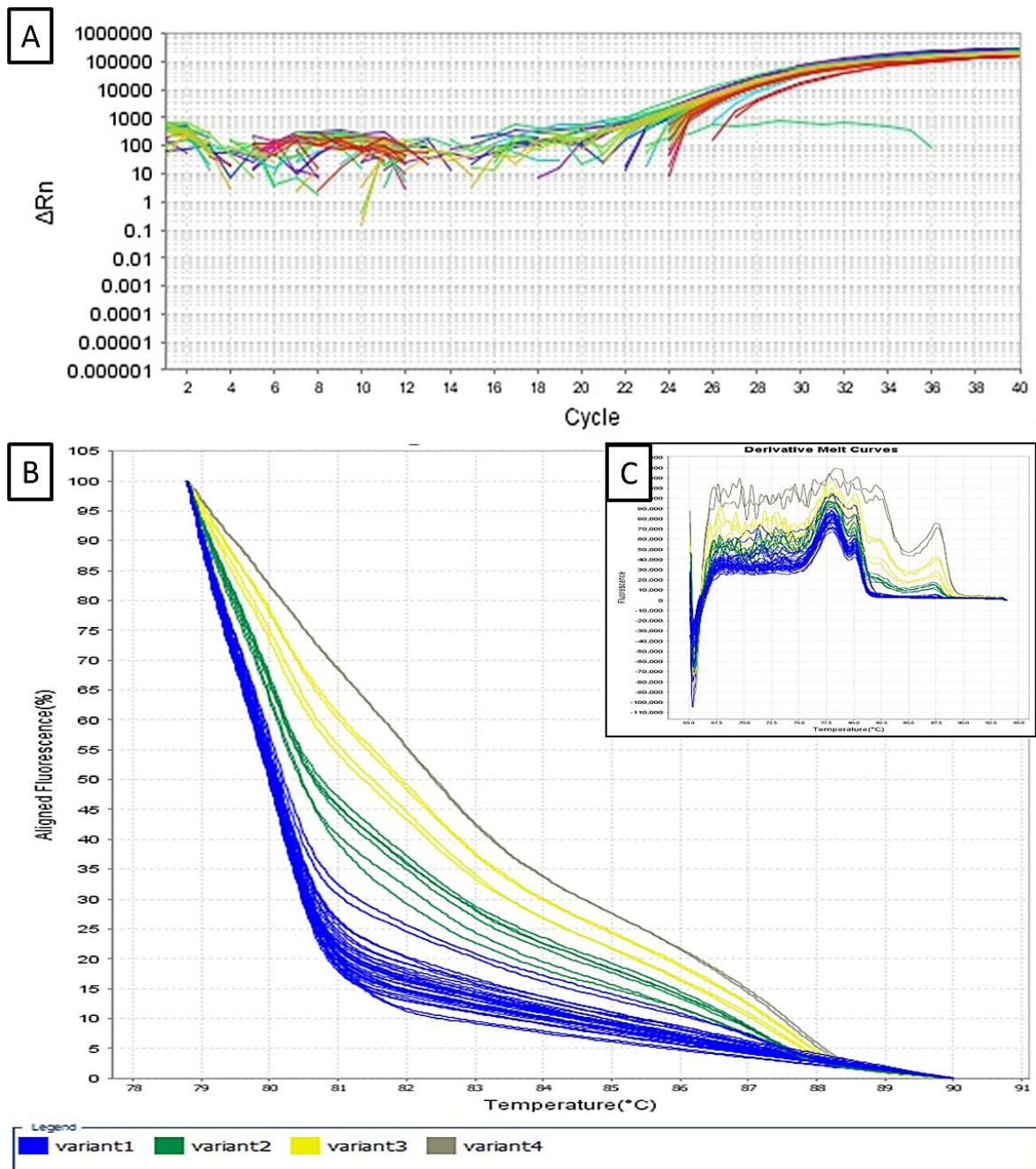


Figure 23 - HRM curve generated by amplification of *APP* region downstream TSS (second primer set). **A** – Amplification plot for samples and methylation DNA controls with each color corresponding to a sample. **B** – Aligned melt curve between 79°C and 89,8°C with samples grouped by variants according with similar melting behavior; **C** – Derivative melt curves showing three main peaks at 77°C, 80°C and 87,5°C, however only the last two having relevance to the study and corresponding to unmethylated and methylated DNA fragment population, respectively. The first peak may result from unspecific product generated in the PCR reaction. No distinction could be observed as both possible AD patients and age- and sex-matched controls localized in the same variants (in detailed at Table 14).

The results of variant calls obtained for HRM are listed in the Table 14. Samples were grouped in each variant according to the similarity of melting profiles. Using this approach no distinction could be made between control and possible AD individuals for the *APP* promoter regions evaluated.

Table 14 – Variant call results from HRM analysis. The Silhouette Scores helped software to determine the variants and it measures the level of sample similarity in each variant according to the melting profile. Samples with similar melting profiles were grouped into the same variant.

Gene	Variant	Samples		Silhouette Scores
<i>ApoE</i>	1	Standards	0% methylated	80,0-99,8
		Samples	D4, C8, C9, D1, C2', D3, D5, D6, D9 and IPC	
	2	Samples	C1, C2, C3, C7, D2, D7 and D8	
	3	Samples	100% methylated	
<i>APP</i> (upstream)	1	Standards	0%, 1%, 3%, 5%	84,0-98,8
	2	Samples	All the samples tested	
	3	Standards	10%, 25%, 100%	
<i>APP</i> (Downstream)	1	Samples	All the samples tested	84,0 – 98,8
	2	Standards	0%, 1%, 3%, 5%	
	3	Standards	10%, 25%	
	4	Standards	100%	

4.3.3. Evaluation of *ApoE* methylation levels by sequencing analysis

Since no differences could be observed for the *APP* promoter region chosen, this approach was only carried out for *ApoE* gene, which revealed minor modifications by COBRA assay. In order to set up the optimal conditions for PCR products, the methylated and unmethylated DNA controls were initially sequenced. After establishing the optimal sequencing conditions, all PCR products were sequenced and analyzed. In all samples, whole methylation percentages for the promoter sequence of *ApoE* were determined, as well as methylation upstream and downstream the TSS. Furthermore, for each sequence the bisulfite conversion efficiency were evaluated, ensuring that all non-methylated cytosines had been converted and ensuring that all sequences could be used for analysis.

Although for the *ApoE* amplified sequence the methylated DNA control had all CpG sites methylated (Figure 24), unmethylated DNA control exhibited almost equal levels of methylation as the methylated one (Figure 25), which can also explain the results obtain in MS-HRM analysis (Figure 21).

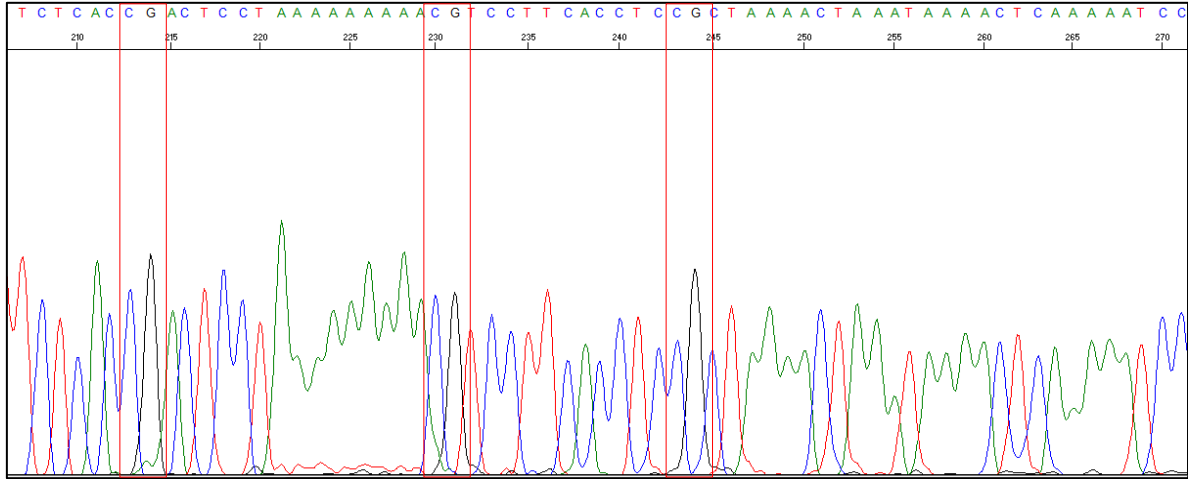


Figure 24 – *ApoE* bisulfite sequencing of methylated DNA control. The sequence represents part of the gene sequence in study (between position –95 and –30 from the TSS). Throughout the bisulfite sequencing, it was possible to observe that all non-methylated cytosines were successfully converted to uracil and that all CpG sites were methylated.

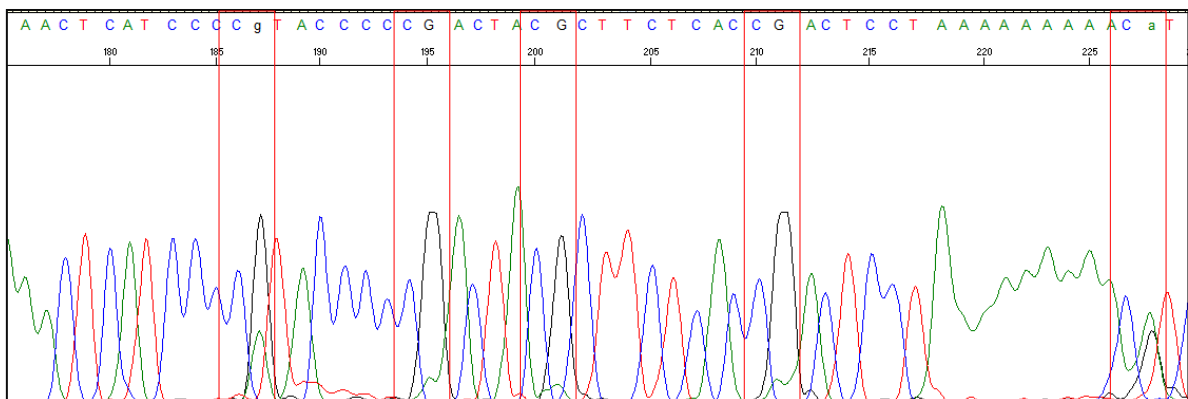


Figure 25 – *ApoE* bisulfite sequencing of unmethylated DNA control. The sequence represents part of the gene sequence in study (between position –55 and –3 according with the TSS). Throughout the bisulfite sequencing, all non-methylated cytosines were successfully converted to uracil. However, CpG sites appeared methylated or 50% methylated indicating that the control is not a true unmethylated control for *ApoE* promoter gene.

The samples were sequenced in the same conditions as the methylation DNA controls but only five samples managed to reach to the end of sequence. All the other samples showed many signal interference that did not allow the electropherogram analysis. Nonetheless, it was possible to sequence the *ApoE* region upstream TSS (Figure 26) for all samples, which include the first 6 CpGs. Qualitative analyses revealed that samples, as already observed in HRM analysis, exhibited low methylation levels, in general below 20% (Figure 26).

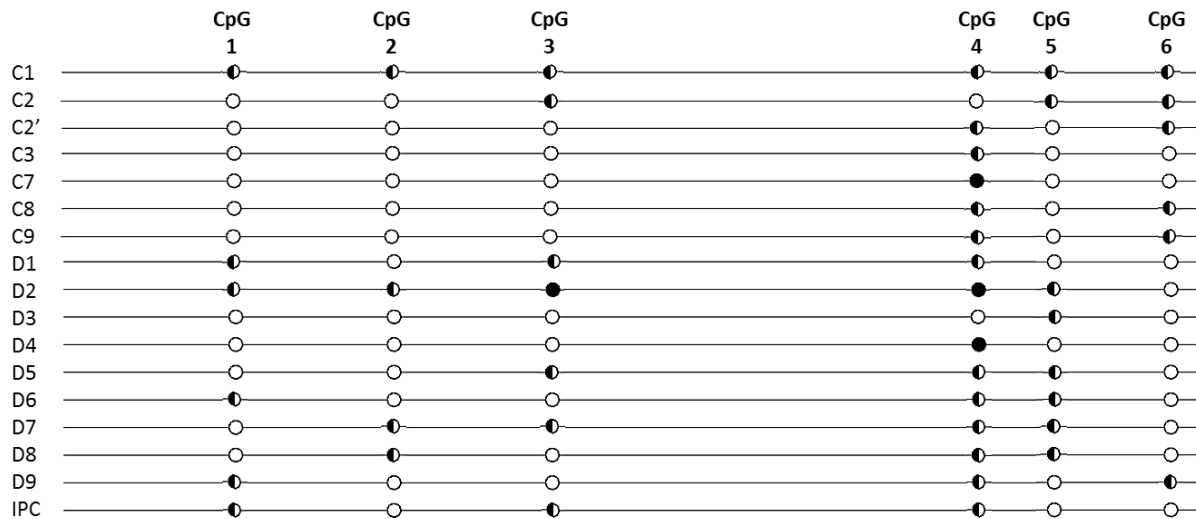


Figure 26 - Results from bisulfite sequencing of APOE upstream TSS region. All circles represent CpG sites in the sequence. Black circles are methylated CpG, half black and half white circles represent partially methylated CpGs; and white ones represent unmethylated CpG.sites.

The semi-quantitative analysis revealed variability between AD patients and age- and sex-matched controls, suggesting, as the techniques used before, that there is not an evident *ApoE* methylation pattern typical of AD patients, at least for the region tested (Table 15). However, and although no clear differences could be observed in the global CpGs methylation levels for this region among age- and sex-matched controls and possible AD individuals (25% *versus* 28%, respectively), differences were detected if we look at the mean values at specific CpG sites. In particular, a tendency to a methylation increase for CpG1, 3 and 5 sites and a marked methylation decrease for CpG6 could be observed for possible AD patients comparatively to control individuals.

Table 15 – Semi-quantitative analysis of CpG sites upstream *ApoE* TSS. The CpG 1, CpG3 and CpG 5 show a tendency for increased methylation level in possible AD patients. On the other hand, CpG 6 exhibited the opposite behavior, with possible AD patients showing increased methylation levels when compared to age- and sex-matched controls.

	Samples	CpG 1	CpG 2	CpG 3	CpG 4	CpG 5	CpG 6	CpG Global Methylation
Age- and sex-matched Controls	C1	24%	23%	30%	72%	27%	68%	41%
	C2	0%	15%	20%	47%	11%	38%	22%
	C2'	0%	0%	15%	67%	21%	60%	27%
	C3	19%	20%	15%	79%	11%	9%	25%
	C7	21%	17%	18%	81%	9%	0%	24%
	C8	0%	0%	18%	55%	0%	37%	18%
	C9	0%	0%	12%	57%	0%	56%	21%
Possible AD Patients	D1	30%	17%	27%	79%	20%	0%	29%
	D2	21%	27%	84%	84%	29%	0%	41%
	D3	20%	16%	19%	16%	79%	0%	25%
	D4	11%	14%	18%	79%	16%	0%	23%
	D5	16%	20%	25%	76%	23%	0%	27%
	D6	24%	14%	16%	72%	23%	11%	27%
	D7	10%	21%	23%	73%	21%	19%	28%
	D8	8%	23%	11%	79%	21%	4%	24%
	D9	26%	17%	10%	54%	20%	34%	27%
	IPC	22%	16%	25%	73%	20%	8%	27%
Means (±SD)	Controls	9% (±0,11)	11% (±0,10)	18% (±0,05)	65% (±0,12)	11% (±0,08)	38% (±0,25)	25% (±0,05)
	Patients	18% (±0,07)	19% (±0,05)	26% (±0,27)	68% (±0,20)	28% (±0,18)	8% (±0,11)	28% (±0,05)

5. Discussion

The DNA methylation is the epigenetic mechanism that has been linked to cancer and recently it is being pointed to have an important role in neurological disorders, including AD. As AD etiology and pathological development is yet to be clarified, epigenetic mechanisms like DNA methylation may underlie the imbalance of protein expression in this disease, such as increase in *APP* and consequently A β production, which along with aggregation of other proteins, lead to the formation of senile plaques, one of the major hallmarks in AD pathology.

In this pilot study, global methylation levels were measured through an ELISA assay. The global methylation percentages results showed that genomic methylation levels, as expected, are very low (below approximately 1%). Global methylation analysis pointed to a hypomethylation in AD patients when compared to age- and sex-matched controls, which can explain the abnormal expression of certain genes due to disruption of its DNA epigenetic control mechanisms. This finding is also in agreement with other studies that report global and gene-specific hypomethylation in AD patients (152–154). However, individually some samples exhibited the opposite behavior either showing equal or increased methylation levels, which can be explained taking into account the clinical history of those patients. The two control-patients pairs that exhibited equal levels of methylation (Figure 16) were C3-D6 and C7-D7 (Table 13). The clinical history of the patient D6 revealed parkinsonism symptoms and treatment for dizziness. Although several studies had reported hypomethylation in Parkinson disease either in brain or blood samples (107,155–157), the treatment for dizziness can mask the true methylation levels of the sample. In another study (158) from our laboratory, carried on the same samples, the D6 patient was also considered an outlier, since it was the only sample that did not fit into the groups generated by multivariate analysis for differentiation of possible AD patients from age- and sex-matched controls, by spectroscopy analysis. On the other hand, D7, besides undergoing the same treatment as C7 for dyslipidemia, had also treatment for hypertension and diabetes. DNA methylation role in hypertension is still not clear (159,160) but in diabetes some genes had been reported as hypermethylated, such as in the case of type 2 diabetes mellitus, either in tissue or blood samples (161,162). These results can explain the equal methylation levels in this control and AD patient. The patient D2 had a global methylation level above the control, which can be explained by the fact that he was being treated for AD, which by itself could induce an increase in the global methylation levels. The patient D9 did not have any history of clinical treatment, unlike its age- and sex-matched control, C9, which was being treated for hypertension and dyslipidemia and therefore, his “true” methylation levels could be also masked by the treatment.

Further, previous studies reported (163–165) that the global methylation levels decreased with age however in our study this correlation was not clear most probably due to the study group size, which needs to be increased.

Besides the global methylation analysis two important genes in AD pathology were studied in order to search for methylation changes in their promoter region among possible AD patients and age- and sex-matched controls. DNA methylation is inversely correlated with gene expression, thus by studying promoter regions, more specifically at TSS region, could give insights about the variability of methylation in these areas and its correlation with gene expression. The genes studied were *APP* and *ApoE*, being that for the former gene, the promoter was localized within a CGI, while for the *ApoE* gene the only CGI was located several bases upstream the promoter. Different techniques were used in order to characterize the methylation in the promoters regions of these genes.

The first technique used to evaluate the methylation levels of AD related genes was COBRA. The aim was to see if any distinctive pattern was visible between age- and sex-matched controls and possible AD patients. For the *APP* promoter region analyzed no differences in the methylation levels could be detected when comparing AD patients with age- and sex-matched controls, as no cleavage products was visible in neither of them. This result suggests the absence of methylation at the sites recognized by the restriction enzyme. On the other hand, *ApoE* promoter exhibited low methylation levels, which is in agreement with the fact that most of the PCR product remained uncutted. The detected methylation pattern was very heterogeneous between age- and sex-matched controls and possible AD patients, with multiple cleavage patterns being detected (Figure 14). This heterogeneity had been also reported by Wang S-C *et al* (101) for the same *ApoE* promoter region herein tested. In the later study a different *ApoE* region was also evaluated and interindividual epigenetic variability was evident.

For *ApoE* promoter gene (Figure 21), MS-HRM experiments used the same set of primers used in COBRA, however, some limitations arise due to the lack of adequate controls. The DNA methylated and unmethylated controls did not allow a correct interpretation of the melting curves since they either had no difference in the melting profile (in the case of *ApoE* study) or had methylation profiles that do not correspond to true unmethylated and methylated DNA controls (in the case of *APP* study). Three different DNA methylation controls under different PCR conditions were tested without any satisfactory results. Although the lack of the appropriate controls, the melting curve analysis for *ApoE* promoter allowed grouping the samples into two variants with different methylation levels (Table 14). Nonetheless, as both variants contained age

and sex-matched controls and possible AD patients no distinct pattern could be identified for those. These results corroborate the ones observed in COBRA assay and suggest a methylation heterogeneity in this promoter region of the gene. The same was observed for APP MS-HRM analysis. All samples exhibited melting curve profiles that indicated levels of methylation below the unmethylated control used, hindering the quantification of samples' methylation levels. However, despite being grouped in the same variant in both regions, upstream and downstream the APP TSS, samples exhibited slightly different melting profiles that suggest low methylation levels that could be correctly quantified by using an appropriate DNA methylation control. Furthermore, in the APP derivative melt curve it is possible to view unspecific products in both experiences (Figure 22–C and Figure 23–C) with the early appearance of multiple temperature melting peaks, indicating that the reaction was not fully optimized. Due to that the melting curve behavior of the samples may vary therefore not allowing the correct analysis by this technique. Thus far, no study had performed MS-HRM for analysis neither for *APP* nor *ApoE* promoter genes. Some studies had pointed to an epigenetic regulation of *APP* expression (166) with some authors reporting hypomethylation in different gene regions such as promoter (167) and exonic (116) regions; while others reported low methylation levels in *APP* promoter region, with no differences between patients and controls (168).

In contrast with *APP*, the *ApoE* gene exhibited minor alterations in methylation levels among controls and patients by COBRA, although their distribution patterns were heterogeneous among samples. Hence, in order to determine if any particular CpG site of *ApoE* promoter region (not possible through COBRA or MS-HRM) was differently methylated in age- and sex-matched controls and possible AD patients, Bisulfite Direct Sequencing, considered the gold-standard for methylation analysis, was carried out. The amplification of *ApoE* for this analysis was successful. Of the total CpG sites, six could be analyzed for all samples when using the reverse internal primer. Analyzing global CpG methylation levels, no differences were observed and the results correlated with the ones verified in MS-HRM. However, comparing the mean levels of controls and possible AD patients, some differences were detected in specific CpG sites (Table 15). In particular, CpG 1, 3 and 5 appeared to show a tendency to be more methylated in AD comparatively to age- and sex-matched controls. On the other hand, CpG 6 showed a decrease in methylation levels for possible AD patients. It would be interesting to confirm these results in a large sample number and to extend this analysis to the 15 CpG sites of *ApoE* promoter region.

CONCLUDING REMARKS

In this study a tendency for a global methylation decrease of possible AD patients was observed when compared to aged- and sex-matched controls. In particular, when addressing the methylation levels of *APP*, a gene linked to AD pathology, and *ApoE*, described as a risk factor to AD, no gene specific methylation differences could be observed between possible AD patients and control individuals, either by COBRA or MS-HRM. However, when looking at specific CpG sites of *ApoE* promoter region by sequencing analysis differences could be detected between age- and sex-matched controls and possible AD patients. Since gene expression can be regulated by epigenetic mechanisms, alterations in the methylation levels may render in imbalanced expression of genes relevant to AD pathology.

STUDIED LIMITATIONS AND FUTURE PERSPECTIVE

The first limitation of this study is related with the number of samples used (below 30). The results obtained for global methylation needs to be confirmed using a large number of samples, including the ones used in this study.

Another important issue lies on the fact that the DNA methylation controls were not the appropriate for MS-HRM analysis and, therefore, could induced bias in the PCR amplification, resulting in inaccurate estimation of methylation levels in COBRA and in bisulfite sequencing (169). In order to address this issue, DNA used should be from a cellular lineage with *APP* and *ApoE* genes unmethylated. The results from *APP* MS-HRM analysis revealed unspecific products that could affect the melting profile of the samples. For the region before *APP* TSS, different conditions were tested but unspecific products had been a constant in every assay. Probably a new set of primers for the same region could yield better results. The same solution could improve the results for the region downstream *APP* TSS.

In the case of bisulfite sequencing, the use of M13-tailed primers can be a solution to obtain *ApoE* complete sequencing in all samples and to analyze the 15 CpGs sites. Furthermore, all samples exhibit some guanine base signal background that could culminate in bias methylation levels. Therefore, the results from bisulfite sequencing need to be confirmed using a different basecaller, such as KB basecaller (Applied Biosystems), which is indicated for bisulfite sequencing analysis. This software was incompatibility to Genetic Analyzer 310 platforms. Furthermore, the results obtained using reverse primer should also be confirmed using forward primer.

Furthermore, in future studies, the methylation levels of other CGI in *APP* and *ApoE* genes, both upstream from the respective promoters, could be evaluated in order to determine if the methylation levels are altered and could have any influence in its gene expression. Furthermore, there are others AD-related genes that may hold interest in evaluate the methylation profile. The genes of presenilin 1 and 2 and *MAPT* gene, which encodes tau protein, one of the major components in the NFTs, can give more insights and help in understanding of the epigenetic changes in AD pathology.

6. References

1. Daniilidou M, Koutroumani M, Tsolaki M. Epigenetic mechanisms in Alzheimer's disease. *Curr. Med. Chem.* 2011/04/07 ed. 2011 Jan;18(12):1751–6.
2. Gräff J, Mansuy IM. Epigenetic dysregulation in cognitive disorders. *Eur. J. Neurosci.* 2009/06/11 ed. 2009 Jul;30(1):1–8.
3. Portela A, Esteller M. Epigenetic modifications and human disease. *Nat. Biotechnol.* 2010/10/15 ed. 2010 Oct;28(10):1057–68.
4. Bonasio R, Tu S, Reinberg D. Molecular signals of epigenetic states. *Science.* 2010/10/30 ed. 2010 Oct 29;330(6004):612–6.
5. Fraga MF, Ballestar E, Paz MF, Ropero S, Setien F, Ballestar ML, et al. Epigenetic differences arise during the lifetime of monozygotic twins. *Proc. Natl. Acad. Sci. U. S. A.* 2005 Jul 26;102(30):10604–9.
6. Meissner A. Epigenetic modifications in pluripotent and differentiated cells. *Nat. Biotechnol.* 2010 Oct;28(10):1079–88.
7. Hernandez DG, Nalls MA, Gibbs JR, Arepalli S, van der Brug M, Chong S, et al. Distinct DNA methylation changes highly correlated with chronological age in the human brain. *Hum. Mol. Genet.* 2011 Mar 15;20(6):1164–72.
8. Numata S, Ye T, Hyde TM, Guitart-Navarro X, Tao R, Wininger M, et al. DNA methylation signatures in development and aging of the human prefrontal cortex. *Am. J. Hum. Genet.* 2012 Feb 10;90(2):260–72.
9. Cheung I, Shulha HP, Jiang Y, Matevossian A, Wang J, Weng Z, et al. Developmental regulation and individual differences of neuronal H3K4me3 epigenomes in the prefrontal cortex. *Proc. Natl. Acad. Sci. U. S. A.* 2010 May 11;107(19):8824–9.
10. Klein CJ, Botuyan M-V, Wu Y, Ward CJ, Nicholson GA, Hammans S, et al. Mutations in DNMT1 cause hereditary sensory neuropathy with dementia and hearing loss. *Nat. Genet.* 2011 Jun;43(6):595–600.
11. Winkelmann J, Lin L, Schormair B, Kornum BR, Faraco J, Plazzi G, et al. Mutations in DNMT1 cause autosomal dominant cerebellar ataxia, deafness and narcolepsy. *Hum. Mol. Genet.* 2012 May 15;21(10):2205–10.
12. Peter CJ, Akbarian S. Balancing histone methylation activities in psychiatric disorders. *Trends Mol. Med.* 2011 Jul;17(7):372–9.
13. Chuang D-M, Leng Y, Marinova Z, Kim H-J, Chiu C-T. Multiple roles of HDAC inhibition in neurodegenerative conditions. *Trends Neurosci.* 2009 Nov;32(11):591–601.
14. Fischer A, Sananbenesi F, Mungenast A, Tsai L-H. Targeting the correct HDAC(s) to treat cognitive disorders. *Trends Pharmacol. Sci.* 2010 Dec;31(12):605–17.
15. Bird A. Perceptions of epigenetics. *Nature.* 2007/05/25 ed. 2007;447(7143):396–8.

16. Ai S, Shen L, Guo J, Feng X, Tang B. DNA methylation as a biomarker for neuropsychiatric diseases. *Int. J. Neurosci.* 2012;122(4):165–76.
17. Gardiner-Garden M, Frommer M. CpG islands in vertebrate genomes. *J. Mol. Biol.* 1987/07/20 ed. 1987 Jul 20;196(2):261–82.
18. Chatterjee R, Vinson C. CpG methylation recruits sequence specific transcription factors essential for tissue specific gene expression. *Biochim. Biophys. Acta - Gene Regul. Mech.* 2012;1819(7):763–70.
19. Bird A. DNA methylation patterns and epigenetic memory. *Genes Dev.* 2002 Jan 1;16(1):6–21.
20. Kaneda M, Okano M, Hata K, Sado T, Tsujimoto N, Li E, et al. Essential role for de novo DNA methyltransferase Dnmt3a in paternal and maternal imprinting. *Nature.* 2004 Jun 24;429(6994):900–3.
21. Bourc'his D, Xu GL, Lin CS, Bollman B, Bestor TH. Dnmt3L and the establishment of maternal genomic imprints. *Science.* 2001 Dec 21;294(5551):2536–9.
22. Howell CY, Bestor TH, Ding F, Latham KE, Mertineit C, Trasler JM, et al. Genomic imprinting disrupted by a maternal effect mutation in the Dnmt1 gene. *Cell.* 2001 Mar 23;104(6):829–38.
23. Reik W. Stability and flexibility of epigenetic gene regulation in mammalian development. *Nature.* 2007/05/25 ed. 2007;447(7143):425–32.
24. Szyf M. Epigenetics, DNA methylation, and chromatin modifying drugs. *Annu Rev Pharmacol Toxicol.* 2008/10/15 ed. 2009;49:243–63.
25. Chen T, Ueda Y, Xie S, Li E. A novel Dnmt3a isoform produced from an alternative promoter localizes to euchromatin and its expression correlates with active de novo methylation. *J Biol Chem.* 2002/07/26 ed. 2002;277(41):38746–54.
26. Scarpa S, Cavallaro RA, D'Anselmi F, Fusco A. Gene silencing through methylation: an epigenetic intervention on Alzheimer disease. *J Alzheimers Dis.* 2006/08/19 ed. 2006;9(4):407–14.
27. Narayan P, Dragunow M. Pharmacology of epigenetics in brain disorders. *Br J Pharmacol.* 2009/12/18 ed. 2010;159(2):285–303.
28. Kuroda A, Rauch TA, Todorov I, Ku HT, Al-Abdullah IH, Kandeel F, et al. Insulin gene expression is regulated by DNA methylation. Maedler K, editor. *PLoS One. Public Library of Science*; 2009 Jan;4(9):e6953.
29. Esteller M. Epigenetic gene silencing in cancer: the DNA hypermethylome. *Hum. Mol. Genet.* 2007 Apr 15;16 Spec No:R50–9.

30. Urdinguio RG, Sanchez-Mut J V, Esteller M. Epigenetic mechanisms in neurological diseases: genes, syndromes, and therapies. *Lancet Neurol.* 2009/10/17 ed. 2009;8(11):1056–72.
31. Wang T, Pan Q, Lin L, Szulwach KE, Song C-X, He C, et al. Genome-wide DNA hydroxymethylation changes are associated with neurodevelopmental genes in the developing human cerebellum. *Hum. Mol. Genet.* 2012/10/09 ed. 2012 Dec 15;21(26):5500–10.
32. Guo JU, Su Y, Zhong C, Ming G, Song H. Hydroxylation of 5-methylcytosine by TET1 promotes active DNA demethylation in the adult brain. *Cell.* Elsevier; 2011 Apr 29;145(3):423–34.
33. Tahiliani M, Koh KP, Shen Y, Pastor WA, Bandukwala H, Brudno Y, et al. Conversion of 5-methylcytosine to 5-hydroxymethylcytosine in mammalian DNA by MLL partner TET1. *Science.* 2009 May 15;324(5929):930–5.
34. Guibert S, Weber M. Functions of DNA methylation and hydroxymethylation in Mammalian development. *Curr Top Dev Biol.* 2013/04/17 ed. 2013;104:47–83.
35. Olkhov-Mitsel E, Bapat B. Strategies for discovery and validation of methylated and hydroxymethylated DNA biomarkers. *Cancer Med.* 2012 Oct;1(2):237–60.
36. Cooper GM, Hausman RE. *The Cell.* Sinauer Associates Inc.,U.S.; 2006. p. 739.
37. Kapranov P. From transcription start site to cell biology. *Genome Biol.* 2009/05/14 ed. 2009;10(4):217.
38. Doi A, Park IH, Wen B, Murakami P, Aryee MJ, Irizarry R, et al. Differential methylation of tissue- and cancer-specific CpG island shores distinguishes human induced pluripotent stem cells, embryonic stem cells and fibroblasts. *Nat Genet.* 2009/11/03 ed. 2009;41(12):1350–3.
39. Sananbenesi F, Fischer A. The epigenetic bottleneck of neurodegenerative and psychiatric diseases. *Biol Chem.* 2009/09/15 ed. 2009;390(11):1145–53.
40. Kouzarides T. Chromatin modifications and their function. *Cell.* 2007 Feb 23;128(4):693–705.
41. Luco RF, Pan Q, Tominaga K, Blencowe BJ, Pereira-Smith OM, Misteli T. Regulation of alternative splicing by histone modifications. *Science.* 2010 Feb 19;327(5968):996–1000.
42. Huertas D, Sendra R, Muñoz P. Chromatin dynamics coupled to DNA repair. *Epigenetics.* 2009 Jan;4(1):31–42.
43. Chouliaras L, Rutten BPF, Kenis G, Peerbooms O, Visser PJ, Verhey F, et al. Epigenetic regulation in the pathophysiology of Alzheimer's disease. *Prog. Neurobiol.* Elsevier Ltd; 2010 Apr;90(4):498–510.

44. Abel T, Zukin RS. Epigenetic targets of HDAC inhibition in neurodegenerative and psychiatric disorders. *Curr Opin Pharmacol*. 2008/01/22 ed. 2008;8(1):57–64.
45. Li B, Carey M, Workman JL. The role of chromatin during transcription. *Cell*. 2007 Feb 23;128(4):707–19.
46. Chodavarapu RK, Feng S, Bernatavichute Y V, Chen P-Y, Stroud H, Yu Y, et al. Relationship between nucleosome positioning and DNA methylation. *Nature*. 2010 Jul 15;466(7304):388–92.
47. Getun I V, Wu ZK, Khalil AM, Bois PRJ. Nucleosome occupancy landscape and dynamics at mouse recombination hotspots. *EMBO Rep. Nature Publishing Group*; 2010 Jul 1;11(7):555–60.
48. Reisman D, Glaros S, Thompson EA. The SWI/SNF complex and cancer. *Oncogene*. 2009 Apr 9;28(14):1653–68.
49. Ho L, Crabtree GR. Chromatin remodelling during development. *Nature*. 2010 Jan 28;463(7280):474–84.
50. Clapier CR, Cairns BR. The biology of chromatin remodeling complexes. *Annu. Rev. Biochem*. 2009 Jan;78:273–304.
51. Yoo AS, Staahl BT, Chen L, Crabtree GR. MicroRNA-mediated switching of chromatin-remodelling complexes in neural development. *Nature*. 2009 Jul 30;460(7255):642–6.
52. Chuang JC, Jones PA. Epigenetics and microRNAs. *Pediatr Res*. 2007/04/07 ed. 2007;61(5 Pt 2):24R–29R.
53. Esquela-Kerscher A, Slack FJ. Oncomirs - microRNAs with a role in cancer. *Nat. Rev. Cancer*. 2006 Apr;6(4):259–69.
54. Meltzer PS. Cancer genomics: Small RNAs with big impacts. *Nature*. 2005 Jun 9;435(7043):745–6.
55. Lewis BP, Shih I, Jones-Rhoades MW, Bartel DP, Burge CB. Prediction of Mammalian MicroRNA Targets. *Cell*. 2003 Dec;115(7):787–98.
56. Lim LP, Lau NC, Garrett-Engle P, Grimson A, Schelter JM, Castle J, et al. Microarray analysis shows that some microRNAs downregulate large numbers of target mRNAs. *Nature*. 2005 Jan 30;433(7027):769–73.
57. Wang Z, Yao H, Lin S, Zhu X, Shen Z, Lu G, et al. Transcriptional and epigenetic regulation of human microRNAs. *Cancer Lett*. 2012/12/19 ed. 2013;331(1):1–10.
58. Saito Y, Liang G, Egger G, Friedman JM, Chuang JC, Coetzee GA, et al. Specific activation of microRNA-127 with downregulation of the proto-oncogene BCL6 by chromatin-modifying drugs in human cancer cells. *Cancer Cell*. 2006 Jun;9(6):435–43.

59. Wutz A, Smrzka OW, Schweifer N, Schellander K, Wagner EF, Barlow DP. Imprinted expression of the Igf2r gene depends on an intronic CpG island. *Nature*. 1997 Oct 16;389(6652):745–9.
60. Crews D. Epigenetics and its implications for behavioral neuroendocrinology. *Front. Neuroendocrinol*. 2008 Jun;29(3):344–57.
61. Babenko O, Kovalchuk I, Metz GA. Epigenetic programming of neurodegenerative diseases by an adverse environment. *Brain Res*. 2012/02/15 ed. 2012;1444:96–111.
62. Ballard C, Gauthier S, Corbett A, Brayne C, Aarsland D, Jones E. Alzheimer's disease. *Lancet*. 2011 Mar 19;377(9770):1019–31.
63. Cummings JL. Alzheimer's disease. *N Engl J Med*. 2004/07/02 ed. 2004;351(1):56–67.
64. McKhann G, Drachman D, Folstein M, Katzman R, Price D, Stadlan EM. Clinical diagnosis of Alzheimer's disease: report of the NINCDS-ADRDA Work Group under the auspices of Department of Health and Human Services Task Force on Alzheimer's Disease. *Neurology*. 1984 Jul;34(7):939–44.
65. Holtzman DM, Morris JC, Goate AM. Alzheimer's disease: the challenge of the second century. *Sci Transl Med*. 2011/04/08 ed. 2011;3(77):77sr1.
66. Bertram L, Tanzi RE. The genetics of Alzheimer's disease. *Prog Mol Biol Transl Sci*. 2012/04/10 ed. 2012;107:79–100.
67. Ray WJ, Ashall F, Goate AM. Molecular pathogenesis of sporadic and familial forms of Alzheimer's disease. *Mol. Med. Today*. 1998 Apr;4(4):151–7.
68. Marques SC, Oliveira CR, Outeiro TF, Pereira CM. Alzheimer's disease: the quest to understand complexity. *J Alzheimers Dis*. 2010/06/18 ed. 2010;21(2):373–83.
69. Ferri CP, Prince M, Brayne C, Brodaty H, Fratiglioni L, Ganguli M, et al. Global prevalence of dementia: a Delphi consensus study. *Lancet*. 2005/12/20 ed. 2005;366(9503):2112–7.
70. Mayeux R, Stern Y. Epidemiology of Alzheimer disease. *Cold Spring Harb Perspect Med*. 2012/08/22 ed. 2012;2(8).
71. Evans DA, Funkenstein HH, Albert MS, Scherr PA, Cook NR, Chown MJ, et al. Prevalence of Alzheimer's disease in a community population of older persons. Higher than previously reported. *JAMA*. 1989/11/10 ed. 1989;262(18):2551–6.
72. Alzheimer Portugal [Internet]. [cited 2013 Jun 13]. Available from: <http://www.alzheimerportugal.org/scid/webAZprt/>
73. Perl DP. Neuropathology of Alzheimer's disease. *Mt Sinai J Med*. 2010/01/27 ed. 2010;77(1):32–42.

74. Serrano-Pozo A, Frosch MP, Masliah E, Hyman BT. Neuropathological alterations in Alzheimer disease. *Cold Spring Harb Perspect Med*. 2012/01/10 ed. 2011;1(1):a006189.
75. Braak H, Braak E. Neuropathological staging of Alzheimer-related changes. *Acta Neuropathol*. 1991 Jan;82(4):239–59.
76. Thal DR, Rüb U, Orantes M, Braak H. Phases of A beta-deposition in the human brain and its relevance for the development of AD. *Neurology*. 2002 Jun 25;58(12):1791–800.
77. Golde TE, Eckman CB, Younkin SG. Biochemical detection of Abeta isoforms: implications for pathogenesis, diagnosis, and treatment of Alzheimer's disease. *Biochim. Biophys. Acta*. 2000 Jul 26;1502(1):172–87.
78. O'Brien RJ, Wong PC. Amyloid precursor protein processing and Alzheimer's disease. *Annu Rev Neurosci*. 2011/04/05 ed. 2011;34:185–204.
79. Bayer TA, Cappai R, Masters CL, Beyreuther K, Multhaup G. It all sticks together--the APP-related family of proteins and Alzheimer's disease. *Mol. Psychiatry*. 1999 Nov;4(6):524–8.
80. Bergmans BA, De Strooper B. gamma-secretases: from cell biology to therapeutic strategies. *Lancet Neurol*. 2010 Feb;9(2):215–26.
81. Zhang YW, Thompson R, Zhang H, Xu H. APP processing in Alzheimer's disease. *Mol Brain*. 2011/01/11 ed. 2011;4:3.
82. Braak E, Braak H, Mandelkow EM. A sequence of cytoskeleton changes related to the formation of neurofibrillary tangles and neuropil threads. *Acta Neuropathol*. 1994 Jan;87(6):554–67.
83. Augustinack JC, Schneider A, Mandelkow E-M, Hyman BT. Specific tau phosphorylation sites correlate with severity of neuronal cytopathology in Alzheimer's disease. *Acta Neuropathol*. 2002 Jan;103(1):26–35.
84. Goate A, Chartier-Harlin MC, Mullan M, Brown J, Crawford F, Fidani L, et al. Segregation of a missense mutation in the amyloid precursor protein gene with familial Alzheimer's disease. *Nature*. 1991 Mar 21;349(6311):704–6.
85. Sherrington R, Rogaev EI, Liang Y, Rogaeva EA, Levesque G, Ikeda M, et al. Cloning of a gene bearing missense mutations in early-onset familial Alzheimer's disease. *Nature*. 1995 Jun 29;375(6534):754–60.
86. Levy-Lahad E, Wijsman EM, Nemens E, Anderson L, Goddard KA, Weber JL, et al. A familial Alzheimer's disease locus on chromosome 1. *Science*. 1995 Aug 18;269(5226):970–3.
87. Schellenberg GD, Montine TJ. The genetics and neuropathology of Alzheimer's disease. *Acta Neuropathol*. 2012;124(3):305–23.
88. Scheuner D, Eckman C, Jensen M, Song X, Citron M, Suzuki N, et al. Secreted amyloid beta-protein similar to that in the senile plaques of Alzheimer's disease is increased in vivo by

- the presenilin 1 and 2 and APP mutations linked to familial Alzheimer's disease. *Nat. Med.* 1996 Aug;2(8):864–70.
89. Strittmatter WJ, Saunders AM, Schmechel D, Pericak-Vance M, Enghild J, Salvesen GS, et al. Apolipoprotein E: high-avidity binding to beta-amyloid and increased frequency of type 4 allele in late-onset familial Alzheimer disease. *Proc. Natl. Acad. Sci. U. S. A.* 1993 Mar 1;90(5):1977–81.
 90. Mahley RW, Rall SC. Is epsilon4 the ancestral human apoE allele? *Neurobiol. Aging.* 20(4):429–30.
 91. Sorbi S, Hort J, Erkinjuntti T, Fladby T, Gainotti G, Gurvit H, et al. EFNS-ENS Guidelines on the diagnosis and management of disorders associated with dementia. *Eur J Neurol.* 2012/08/16 ed. 2012;19(9):1159–79.
 92. Eschweiler GW, Leyhe T, Kloppel S, Hull M. New developments in the diagnosis of dementia. *Dtsch Arztebl Int.* 2010/10/22 ed. 2010;107(39):677–83.
 93. Sheehan B. Assessment scales in dementia. *Ther Adv Neurol Disord.* 2012/11/10 ed. 2012;5(6):349–58.
 94. Yesavage JA, Brink TL, Rose TL, Lum O, Huang V, Adey M, et al. Development and validation of a geriatric depression screening scale: a preliminary report. *J. Psychiatr. Res.* 17(1):37–49.
 95. De Deyn PP, Engelborghs S, Saerens J, Goeman J, Marien P, Maertens K, et al. The Middelheim Frontality Score: a behavioural assessment scale that discriminates frontotemporal dementia from Alzheimer's disease. *Int J Geriatr Psychiatry.* 2004/12/04 ed. 2005;20(1):70–9.
 96. Agosta F, Caso F, Filippi M. Dementia and neuroimaging. *J Neurol.* 2012/12/18 ed. 2013;260(2):685–91.
 97. Zetterberg H, Mattsson N, Blennow K. Cerebrospinal fluid analysis should be considered in patients with cognitive problems. *Int J Alzheimers Dis.* 2010/01/01 ed. 2010;2010:163065.
 98. Xu Z, Li X. DNA Methylation in Neurodegenerative Disorders. *Curr. Transl. Geriatr. Gerontol. Reports.* Current Science Inc.; 2012;1(4):199–205.
 99. Petronis A. Epigenetics as a unifying principle in the aetiology of complex traits and diseases. *Nature.* 2010 Jun 10;465(7299):721–7.
 100. Heyn H, Li N, Ferreira HJ, Moran S, Pisano DG, Gomez A, et al. Distinct DNA methylomes of newborns and centenarians. *Proc. Natl. Acad. Sci. U. S. A.* 2012 Jun 26;109(26):10522–7.
 101. Wang S-C, Oelze B, Schumacher A. Age-Specific Epigenetic Drift in Late-Onset Alzheimer's Disease. *PLoS One.* Public Library of Science; 2008;3(7):e2698.

102. Kennedy BP, Bottiglieri T, Arning E, Ziegler MG, Hansen LA, Masliah E. Elevated S-adenosylhomocysteine in Alzheimer brain: influence on methyltransferases and cognitive function. *J. Neural Transm.* 2004 Apr;111(4):547–67.
103. Fusco A, Seminara L, Cavallaro RA, D'Anselmi F, Scarpa S. S-adenosylmethionine/homocysteine cycle alterations modify DNA methylation status with consequent deregulation of PS1 and BACE and beta-amyloid production. *Mol Cell Neurosci.* 2004/12/21 ed. 2005;28(1):195–204.
104. Tohgi H, Utsugisawa K, Nagane Y, Yoshimura M, Genda Y, Ukitsu M. Reduction with age in methylcytosine in the promoter region -224 approximately -101 of the amyloid precursor protein gene in autopsy human cortex. *Brain Res Mol Brain Res.* 1999/07/17 ed. 1999;70(2):288–92.
105. Oliveira AM, Hemstedt TJ, Bading H. Rescue of aging-associated decline in Dnmt3a2 expression restores cognitive abilities. *Nat Neurosci.* 2012/07/04 ed. 2012;15(8):1111–3.
106. Silva PN, Giguek CO, Leal MF, Bertolucci PH, de Labio RW, Payao SL, et al. Promoter methylation analysis of SIRT3, SMARCA5, HERT and CDH1 genes in aging and Alzheimer's disease. *J Alzheimers Dis.* 2008/04/01 ed. 2008;13(2):173–6.
107. Mastroeni D, Grover A, Delvaux E, Whiteside C, Coleman PD, Rogers J. Epigenetic changes in Alzheimer's disease: decrements in DNA methylation. *Neurobiol Aging.* 2009/01/02 ed. 2010;31(12):2025–37.
108. Mastroeni D, McKee A, Grover A, Rogers J, Coleman PD. Epigenetic differences in cortical neurons from a pair of monozygotic twins discordant for Alzheimer's disease. *PLoS One.* 2009/08/13 ed. 2009;4(8):e6617.
109. Mastroeni D, Grover A, Delvaux E, Whiteside C, Coleman PD, Rogers J. Epigenetic mechanisms in Alzheimer's disease. *Neurobiol Aging.* 2011/04/13 ed. 2011;32(7):1161–80.
110. Wagner PD, Verma M, Srivastava S. Challenges for biomarkers in cancer detection. *Ann N Y Acad Sci.* 2004/07/15 ed. 2004;1022:9–16.
111. Li L, Choi JY, Lee KM, Sung H, Park SK, Oze I, et al. DNA methylation in peripheral blood: a potential biomarker for cancer molecular epidemiology. *J Epidemiol.* 2012/08/07 ed. 2012;22(5):384–94.
112. Choi JY, James SR, Link PA, McCann SE, Hong CC, Davis W, et al. Association between global DNA hypomethylation in leukocytes and risk of breast cancer. *Carcinogenesis.* 2009/07/09 ed. 2009;30(11):1889–97.
113. Moore LE, Pfeiffer RM, Poscablo C, Real FX, Kogevinas M, Silverman D, et al. Genomic DNA hypomethylation as a biomarker for bladder cancer susceptibility in the Spanish Bladder Cancer Study: a case-control study. *Lancet Oncol.* 2008/03/15 ed. 2008;9(4):359–66.

114. Lim U, Flood A, Choi SW, Albanes D, Cross AJ, Schatzkin A, et al. Genomic methylation of leukocyte DNA in relation to colorectal adenoma among asymptomatic women. *Gastroenterology*. 2008/01/02 ed. 2008;134(1):47–55.
115. Widschwendter M, Apostolidou S, Raum E, Rothenbacher D, Fiegl H, Menon U, et al. Epigenotyping in peripheral blood cell DNA and breast cancer risk: a proof of principle study. *PLoS One*. 2008/07/17 ed. 2008;3(7):e2656.
116. West RL, Lee JM, Maroun LE. Hypomethylation of the amyloid precursor protein gene in the brain of an Alzheimer's disease patient. *J Mol Neurosci*. 1995/01/01 ed. 1995;6(2):141–6.
117. Maeda T, Guan JZ, Oyama J, Higuchi Y, Makino N. Aging-associated alteration of subtelomeric methylation in Parkinson's disease. *J Gerontol A Biol Sci Med Sci*. 2009/06/09 ed. 2009;64(9):949–55.
118. Liggett T, Melnikov A, Tilwalli S, Yi Q, Chen H, Replogle C, et al. Methylation patterns of cell-free plasma DNA in relapsing-remitting multiple sclerosis. *J Neurol Sci*. 2010/01/13 ed. 2010;290(1-2):16–21.
119. Ito S, Shen L, Dai Q, Wu SC, Collins LB, Swenberg JA, et al. Tet proteins can convert 5-methylcytosine to 5-formylcytosine and 5-carboxylcytosine. *Science*. 2011 Sep 2;333(6047):1300–3.
120. Egger G, Liang G, Aparicio A, Jones PA. Epigenetics in human disease and prospects for epigenetic therapy. *Nature*. 2004/05/28 ed. 2004;429(6990):457–63.
121. Bolden JE, Peart MJ, Johnstone RW. Anticancer activities of histone deacetylase inhibitors. *Nat Rev Drug Discov*. 2006/09/07 ed. 2006;5(9):769–84.
122. Lane AA, Chabner BA. Histone deacetylase inhibitors in cancer therapy. *J Clin Oncol*. 2009/10/15 ed. 2009;27(32):5459–68.
123. Simonini M V, Camargo LM, Dong E, Maloku E, Veldic M, Costa E, et al. The benzamide MS-275 is a potent, long-lasting brain region-selective inhibitor of histone deacetylases. *Proc Natl Acad Sci U S A*. 2006/01/25 ed. 2006;103(5):1587–92.
124. Alarcon JM, Malleret G, Touzani K, Vronskaya S, Ishii S, Kandel ER, et al. Chromatin acetylation, memory, and LTP are impaired in CBP[±] mice: a model for the cognitive deficit in Rubinstein-Taybi syndrome and its amelioration. *Neuron*. 2004/06/23 ed. 2004;42(6):947–59.
125. Fischer A, Sananbenesi F, Wang X, Dobbin M, Tsai LH. Recovery of learning and memory is associated with chromatin remodelling. *Nature*. 2007/05/01 ed. 2007;447(7141):178–82.
126. Nguyen CT, Weisenberger DJ, Velicescu M, Gonzales FA, Lin JCY, Liang G, et al. Histone H3-Lysine 9 Methylation Is Associated with Aberrant Gene Silencing in Cancer Cells and Is Rapidly Reversed by 5-Aza-2'-deoxycytidine. *Cancer Res*. 2002 Nov 15;62(22):6456–61.

127. Jones PA, Taylor SM. Cellular differentiation, cytidine analogs and DNA methylation. *Cell*. 1980/05/01 ed. 1980;20(1):85–93.
128. Kuendgen A, Lubbert M. Current status of epigenetic treatment in myelodysplastic syndromes. *Ann Hematol*. 2008/04/09 ed. 2008;87(8):601–11.
129. Cheng JC, Matsen CB, Gonzales FA, Ye W, Greer S, Marquez VE, et al. Inhibition of DNA methylation and reactivation of silenced genes by zebularine. *J Natl Cancer Inst*. 2003/03/06 ed. 2003;95(5):399–409.
130. Martinet N, Michel BY, Bertrand P, Benhida R. Small molecules DNA methyltransferases inhibitors. *Medchemcomm*. Royal Society of Chemistry; 2011 Mar 1;3(3):263.
131. Levenson JM, Roth TL, Lubin FD, Miller CA, Huang IC, Desai P, et al. Evidence that DNA (cytosine-5) methyltransferase regulates synaptic plasticity in the hippocampus. *J Biol Chem*. 2006/04/12 ed. 2006;281(23):15763–73.
132. Payao SL, Smith MD, Bertolucci PH. Differential chromosome sensitivity to 5-azacytidine in Alzheimer's disease. *Gerontology*. 1998/08/07 ed. 1998;44(5):267–71.
133. Kim HS, Kim EM, Kim NJ, Chang KA, Choi Y, Ahn KW, et al. Inhibition of histone deacetylation enhances the neurotoxicity induced by the C-terminal fragments of amyloid precursor protein. *J Neurosci Res*. 2003/12/23 ed. 2004;75(1):117–24.
134. Chandra V, Ganguli M, Pandav R, Johnston J, Belle S, DeKosky ST. Prevalence of Alzheimer's disease and other dementias in rural India: the Indo-US study. *Neurology*. 1998/10/22 ed. 1998;51(4):1000–8.
135. Chandra V, Pandav R, Dodge HH, Johnston JM, Belle SH, DeKosky ST, et al. Incidence of Alzheimer's disease in a rural community in India: the Indo-US study. *Neurology*. 2001/09/26 ed. 2001;57(6):985–9.
136. Ishrat T, Hoda MN, Khan MB, Yousuf S, Ahmad M, Khan MM, et al. Amelioration of cognitive deficits and neurodegeneration by curcumin in rat model of sporadic dementia of Alzheimer's type (SDAT). *Eur Neuropsychopharmacol*. 2009/03/31 ed. 2009;19(9):636–47.
137. Brueckner B, Garcia Boy R, Siedlecki P, Musch T, Kliem HC, Zielenkiewicz P, et al. Epigenetic reactivation of tumor suppressor genes by a novel small-molecule inhibitor of human DNA methyltransferases. *Cancer Res*. 2005 Jul 15;65(14):6305–11.
138. Siedlecki P, Garcia Boy R, Musch T, Brueckner B, Suhai S, Lyko F, et al. Discovery of two novel, small-molecule inhibitors of DNA methylation. *J. Med. Chem*. 2006 Jan 26;49(2):678–83.
139. Hughes CP, Berg L, Danziger WL, Coben LA, Martin RL. A new clinical scale for the staging of dementia. *Br. J. Psychiatry*. 1982 Jun;140:566–72.

140. Marshall GA, Rentz DM, Frey MT, Locascio JJ, Johnson KA, Sperling RA. Executive function and instrumental activities of daily living in mild cognitive impairment and Alzheimer's disease. *Alzheimers. Dement.* 2011 May;7(3):300–8.
141. Folstein MF, Folstein SE, McHugh PR. "Mini-mental state." *J. Psychiatr. Res.* 1975;12(3):189–98.
142. Mitchell AJ, Bird V, Rizzo M, Meader N. Diagnostic validity and added value of the Geriatric Depression Scale for depression in primary care: a meta-analysis of GDS30 and GDS15. *J. Affect. Disord.* 2010 Sep;125(1-3):10–7.
143. Mendonça A de; G. Escalas e Testes na Demência. Grupo de Estudos de Envelhecimento Cerebral e Demência - GEECD. 2nd ed. 2008.
144. Patterson K, Molloy L, Qu W, Clark S. DNA methylation: bisulphite modification and analysis. *J Vis Exp.* 2011/11/02 ed. 2011;(56).
145. Bisulfite conversion of DNA for methylation finemapping [Internet]. [cited 2013 Jun 4]. Available from: <http://www.methylogix.com/genetics/protocols.shtml-Dateien/schumachersguide1.html>
146. Salbaum JM, Weidemann A, Lemaire HG, Masters CL, Beyreuther K. The promoter of Alzheimer's disease amyloid A4 precursor gene. *EMBO J.* 1988/09/01 ed. 1988;7(9):2807–13.
147. Paik YK, Chang DJ, Reardon CA, Davies GE, Mahley RW, Taylor JM. Nucleotide sequence and structure of the human apolipoprotein E gene. *Proc Natl Acad Sci U S A.* 1985/05/01 ed. 1985;82(10):3445–9.
148. Lee PY, Costumbrado J, Hsu CY, Kim YH. Agarose gel electrophoresis for the separation of DNA fragments. *J Vis Exp.* 2012/05/02 ed. 2012;(62).
149. Crook R, Hardy J, Duff K. Single-day apolipoprotein E genotyping. *J Neurosci Methods.* 1994/08/01 ed. 1994;53(2):125–7.
150. Wojdacz TK, Dobrovic A. Methylation-sensitive high resolution melting (MS-HRM): a new approach for sensitive and high-throughput assessment of methylation. *Nucleic Acids Res.* 2007 Jan;35(6):e41.
151. Li Y, Tollefsbol TO. DNA methylation detection: bisulfite genomic sequencing analysis. *Methods Mol. Biol.* 2011 Jan;791:11–21.
152. Chouliaras L, Mastroeni D, Delvaux E, Grover A, Kenis G, Hof PR, et al. Consistent decrease in global DNA methylation and hydroxymethylation in the hippocampus of Alzheimer's disease patients. *Neurobiol. Aging.* 2013 Apr 9;34(9):2099–2091.
153. West R, Lee J, Maroun L. Hypomethylation of the amyloid precursor protein gene in the brain of an alzheimer's disease patient. *J. Mol. Neurosci. Humana Press Inc.;* 1995;6(2):141–6.

154. Bollati V, Galimberti D, Pergoli L, Dalla Valle E, Barretta F, Cortini F, et al. DNA methylation in repetitive elements and Alzheimer disease. *Brain Behav Immun.* 2011/02/08 ed. 2011;25(6):1078–83.
155. Kaut O, Schmitt I, Wüllner U. Genome-scale methylation analysis of Parkinson's disease patients' brains reveals DNA hypomethylation and increased mRNA expression of cytochrome P450 2E1. *Neurogenetics.* 2012 Mar;13(1):87–91.
156. Obeid R, Schadt A, Dillmann U, Kostopoulos P, Fassbender K, Herrmann W. Methylation status and neurodegenerative markers in Parkinson disease. *Clin Chem.* 2009/08/15 ed. 2009;55(10):1852–60.
157. Masliah E, Dumaop W, Galasko D, Desplats P. Distinctive patterns of DNA methylation associated with Parkinson disease: Identification of concordant epigenetic changes in brain and peripheral blood leukocytes. *Epigenetics.* 2013 Aug 1;8(10).
158. Silva R. Identification of Alzheimer biomarkers by FTIR – a pilot study. University of Aveiro; 2013.
159. Smolarek I, Wyszko E, Barciszewska AM, Nowak S, Gawronska I, Jablecka A, et al. Global DNA methylation changes in blood of patients with essential hypertension. *Med. Sci. Monit.* 2010 Mar;16(3):CR149–155.
160. Wang X, Falkner B, Zhu H, Shi H, Su S, Xu X, et al. A genome-wide methylation study on essential hypertension in young African American males. *PLoS One.* 2013 Jan;8(1):e53938.
161. Zou L, Yan S, Guan X, Pan Y, Qu X. Hypermethylation of the PRKCZ Gene in Type 2 Diabetes Mellitus. *J. Diabetes Res.* 2013 Jan;2013:721493.
162. Yang BT, Dayeh TA, Volkov PA, Kirkpatrick CL, Malmgren S, Jing X, et al. Increased DNA methylation and decreased expression of PDX-1 in pancreatic islets from patients with type 2 diabetes. *Mol. Endocrinol.* 2012 Jul 8;26(7):1203–12.
163. Wilson VL, Smith RA, Ma S, Cutler RG. Genomic 5-methyldeoxycytidine decreases with age. *J. Biol. Chem.* 1987 Jul 25;262(21):9948–51.
164. Wilson VL, Jones PA. DNA methylation decreases in aging but not in immortal cells. *Science.* 1983 Jun 3;220(4601):1055–7.
165. Drinkwater RD, Blake TJ, Morley AA, Turner DR. Human lymphocytes aged in vivo have reduced levels of methylation in transcriptionally active and inactive DNA. *Mutat. Res.* 1989 Jan;219(1):29–37.
166. Sung HY, Choi EN, Ahn Jo S, Oh S, Ahn JH. Amyloid protein-mediated differential DNA methylation status regulates gene expression in Alzheimer's disease model cell line. *Biochem Biophys Res Commun.* 2011/10/18 ed. 2011;414(4):700–5.

167. Hou Y, Chen H, He Q, Jiang W, Luo T, Duan J, et al. Changes in methylation patterns of multiple genes from peripheral blood leucocytes of Alzheimer's disease patients. *Acta Neuropsychiatr.* 2012;
168. Barrachina M, Ferrer I. DNA methylation of Alzheimer disease and tauopathy-related genes in postmortem brain. *J Neuropathol Exp Neurol.* 2009/07/17 ed. 2009;68(8):880–91.
169. Warnecke PM, Stirzaker C, Melki JR, Millar DS, Paul CL, Clark SJ. Detection and measurement of PCR bias in quantitative methylation analysis of bisulphite-treated DNA. *Nucleic Acids Res.* 1997 Nov 1;25(21):4422–6.

7. Annexes

This section presents the equipment and composition of solutions used for the different techniques applied.

I. Genomic DNA Extraction

- a. Equipment
 - i. Centrifuge 5417R (Eppendorf)
 - ii. Thermomixer comfort (Eppendorf)
- b. Reagents
 - i. QIAamp DNA Blood Mini Kit (Qiagen)
 - ii. RNase A (Sigma-Aldrich)

II. Bisulfite DNA modification

- a. Equipment
 - i. Centrifuge 5417R (Eppendorf)
 - ii. My Cyclor TM (Bio-Rad)
- b. Reagents
 - i. EZ DNA Methylation-Gold Kit (Zymo Research)

III. Global methylation analysis

- a. Equipment
 - i. Infinite M200 (TECAN)
- b. Reagents
 - i. Methylated Quantification Kit (Abnova)

IV. COBRA

- a. Equipment
 - i. My Cyclor TM (Bio-Rad)
 - ii. DNA electrophoresis system (Bio-Rad)
 - iii. Power PAC300 (Bio-Rad)
 - iv. Gel Doc XR System (Bio-Rad).
- b. Reagents
 - i. Maxima Hot Start Master Mix (Thermo Scientific)
 - ii. KAPA HiFi Uracil+ Master Mix (GRISP)
 - iii. HhaI (Thermo Scientific)
 - iv. SsiI (Thermo Scientific)
 - v. 10x Buffer Tango (Thermo Scientific)
 - vi. 10x Buffer O (Thermo Scientific)

- vii. Agarose (Eurobio)
- viii. GreenSafe (NZYTech)
- ix. 0,5M Ethylenediamine tetra-acetic acid (EDTA) (pH 8.0)
 - 1. To 200ml of deionized H₂O add:
 - a. 46,52g EDTA
 - 2. Mix until the solute has dissolved and adjust pH to 8.0 using NaOH.
 - 3. Adjust the volume to 250ml with deionized H₂O.
 - 4. Autoclave solution.
- x. 50x Tris-Acetate-EDTA (TAE) Buffer
 - 1. To 600 ml of deionized H₂O add
 - a. 242g Tris Base
 - b. 57,1ml Glacial Acetic Acid
 - c. 100ml 0,5M EDTA (pH 8.0)
 - 2. Mix until homogenous solution and adjust the volume to 1L with deionized H₂O. Store at room temperature.
- xi. 1 Kb plus DNA ladder (Invitrogen)
- xii. GRS Low Range Ladder (GRISP)
- xiii. SGTB Buffer (GRISP)

V. MS-HRM

- a. Equipment
 - i. StepOnePlus Real-Time PCR System (Applied Biosystems)
- b. Software
 - i. Methyl Primer Express V1.0
 - ii. StepOne Software V2.2.2
 - iii. High Resolution Melt Software v3.0.1 (Applied Biosystems)
- c. Reagents
 - i. MeltDoctor™ HRM Master Mix (Life Technologies)
 - ii. CpGenome™ Human Methylated & Non-Methylated DNA Standard Set

VI. Direct Bisulfite Sequencing

- a. Equipment
 - i. ABI PRISM™ Genetic Analyzer 310

- b. Software
 - i. Sequencing Analysis Software V 3.4.1
 - ii. Sequence Scanner 2
- c. Reagents
 - i. QIAquick PCR purification
 - ii. Ethanol 100%
 - iii. Ethanol 70%
 - iv. sodium acetate 3M pH 5.2